Garamaudo bauciensis*, a new freshwater Mosasauridae (Reptilia, Squamata) from the Santonian (Late Cretaceous) of Provence, southeastern France*

Bardet Nathalie[1*], Houssaye Alexandra[2*], Pelissier François-Louis[3], Dutour Yves[4], Turini Eric[4], Tortosa Thierry[5]

[1] CR2P, Centre de Recherche en Paléontologie – Paris, UMR 7207 CNRS/MNHN/SU, Muséum National d'Histoire Naturelle, CP38, 57 rue Cuvier, 75005 Paris, France
[2] MECADEV, Mécanismes adaptatifs et Evolution, UMR 7179 CNRS/MNHN, Muséum National d'Histoire Naturelle, CP55, 57 rue Cuvier, 75005 Paris, France
[3] Muséum départemental du Var, 737 Chemin du Jonquet, 83000 Toulon, France
[4] Muséum d'Histoire Naturelle, Parc Saint Mitre, 166 Avenue Jean Monnet, 13090 Aix-en-Provence, France
[5] Réserve Naturelle Nationale Sainte-Victoire, Direction de l'Environnement, des Grands Projets et de la Recherche du Département des Bouches-du-Rhône, 52 avenue de Saint-Just, 13256 Marseille Cedex 20, France

[*]Corresponding authors: Nathalie BARDET and Alexandra HOUSSAYE
Correspondence: nathalie.bardet@mnhn.fr, houssaye@mnhn.fr

ABSTRACT

Mosasauroids are primarily known as aquatic squamates that diversified in the marine realm during the Late Cretaceous. While most species had paddles, elongated skull, body, and a laterally compressed tail, and lived in the open sea, some early species, with limbs similar to those of terrestrial animals and a varanoid-like body, lived in marine coastal shallow waters. Recently, mosasauroid remains have been discovered in freshwater environments in several continental deposits of the Santonian-Campanian of Europe. This study describes new cranial and postcranial mosasauroid remains from Santonian continental deposits in Provence, southeastern France, and attributes them to a new tethysaurine: *Garamaudo bauciensis* nov. gen., nov. sp. This mosasauroid, approximately 2.5 m long, with

terrestrial-like limbs and a sacrum, and with osteosclerosis in its vertebrae and humerus (at least), was probably hovering at shallow depth in freshwater ecosystems. This new discovery raises the fact that, according to current knowledge, it is only within the Tethysaurinae that freshwater forms evolved, pointing to a possible niche partitioning, associated with of the maintain of the plesiopedal / plesiopelvic condition, in parallel with the invasion of open waters by most other hydropedal and hydropelvic mosasauroids. This therefore suggests for mosasauroids a richer evolutionary history than currently assumed.

Keywords: Mosasauroidea, Tethysaurinae, new taxon, Late Cretaceous, Freshwater environment, Southern France.

Introduction

Mosasauroidea are an extinct group of aquatic squamates that invaded and diversified in the aquatic environment at the beginning of the Cenomanian, spreading worldwide from the Santonian to the end of the Maastrichtian, and becoming extinct during the biological crisis of the K/Pg boundary (e.g. Bardet *et al.*, 2014; Polcyn *et al.*, 2014). They are usually regarded as toxicoferans (Toxicofera including Anguimorpha, Iguania, Serpentes and all taxa closer to these taxa than to other squamates), and either as the sister group of Varanoidea (Polcyn *et al.*, 2022) or Serpentes (Simoes *et al.*, 2021). Mosasauroidea show elongated skull and body, and a long laterally compressed tail. They encompass a high diversity in size, from 1 to 15 m in length, in ecology, from freshwater, shallow marine to open waters, and in diet, from mollusks and arthropods to large reptiles, through squids and fish (e.g. Bardet *et al.*, 2025).

Most mosasauroids display a morphology strongly modified for an aquatic lifestyle, with paddles and the loss of connection between the vertebral column and the pelvis, that is the absence of a true sacrum. This corresponds to the so-called hydropedal and hydropelvic grade (Caldwell & Palci, 2007). Conversely, more primitive forms display terrestrial-like limbs and a sacrum, illustrating a plesiopedal and plesiopelvic condition. An intermediary pattern with plesiopedal limbs but no sacrum illustrates a third ecological grade.

Most mosasauroid remains are from marine deposits. However, a few taxa and undetermined mosasauroid remains have been encountered in freshwater environments, such as shallow estuarine and fluvial deposits (Holmes *et al.*, 1999), noteworthy in the Santonian-Campanian continental deposits of Europe, from Portugal to Hungary and Austria, passing from southern France (Makádi *et al.*, 2012; Garcia *et al.*, 2015; Ősi *et al.*, 2019, 2021).

This study focuses on new mosasauroid remains discovered in Santonian continental deposits of Provence, southeastern France. These deposits are geographically and stratigraphically close with those where was discovered the Villeveyrac mosasauroid in the lower Campanian of Languedoc, southern France (Garcia *et al.*, 2015). This work proposes the description of this new material and its phylogenetic analysis, to determine its taxonomical and phylogenetic position and whether it represents a new taxon, as well as the description of the geological context coupled with the microanatomical study of some of the bones, in order to characterize its paleobiology and paleoecology.

Geological context

The Bouc-Bel-Air - Sousquières (named along BBAS) locality (Figure 1) is situated along the departmental road RD8, in the city of Bouc-Bel-Air (Bouches-du-Rhône Department, Provence, southeastern France). It lies in the central part of the Aix-en-Provence sedimentary Basin, a broad east–west-oriented syncline formed in a context of Pyrenean-Provençal subsidence during the Late Cretaceous (Guieu, 1968; Gaviglio, 1985; Tortosa & Leleu, 2021).

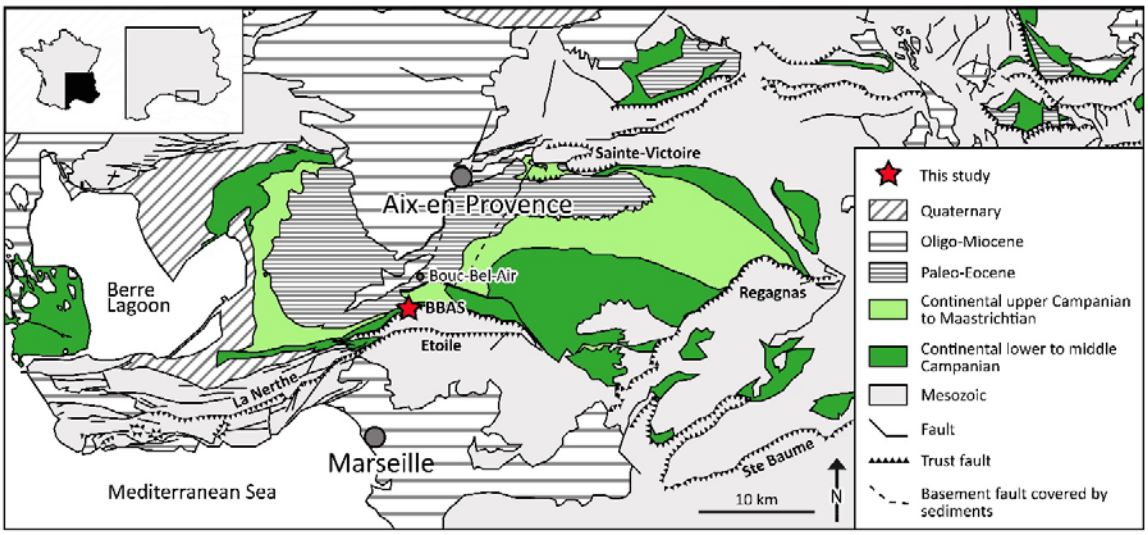

Figure 1. Geographical location of the Bouc-Bel-Air - Sousquières (BBAS) outcrop in the framework of the Upper Cretaceous continental deposits of the Aix-en-Provence Basin, Provence, southeastern France (after Tortosa *et al.*, 2014).

The formations in this area belong to the fluvio-lacustrine complex deposited under a compressive Campanian setting (Gaviglio, 1985; Guieu, 1968). Two basal lithostratigraphic units compose the continental Campanian–Maastrichtian succession: the Valdonnian and the Fuvelian, both historically regarded as local stratigraphic stages (Figure 2C; Matheron, 1878; Collot, 1890; Babinot & Durand, 1980). This area, located along the so-called “Plan-de-Campagne – Bouc-Bel-Air flexure” has only been studied in an unpublished work by Honoré (1938), who described a reference section in the La Malle sector (~2.8 km to the southwest).

The BBAS outcrop is rather limited in size but characteristic with its alternations of beige to brown marls and grey lacustrine limestone beds (Figure 2A, D). Fossils are concentrated at the base of the limestones, at the contact with the marls, which are rich in organic matter and lacustrine mollusk shells, typical of the Valdonnian–Fuvelian assemblages (Figure 2B). These include the bivalve *Corbicula concinna* and the gastropods *Hadraxon acicula* and *Viviparus bosquiana* (Matheron, 1842; Honoré, 1938; Fabre-Taxy, 1951). To these species can be added *Melania colloti* (Roule, 1886; Fabre-Taxy, 1951), only known from the Valdonnian. Another unpublished form is recognized under the name “*Melania vasseuri*“ (Honoré, 1938) and was previously misidentified as *M. praelonga* in Cavin *et al.* (2020). This latter taxon is so far known only from the levels of La Malle and Sousquières (TT., pers. obs.).

The associated vertebrate assemblage includes the actinopterygian *Atractosteus* cf. *africanus* (Cavin *et al*., 1996), the mawsoniid coelacanth *Axelrodichthys megadromos* (Cavin *et al*., 2020), a mosasauroid (this study), the bothremydid turtle *cf. Polysternon sp.*, indeterminate crocodylomorphs and the dromaeosaurid *Richardoestesia* cf*. gilmorei* (TT., pers. obs.).

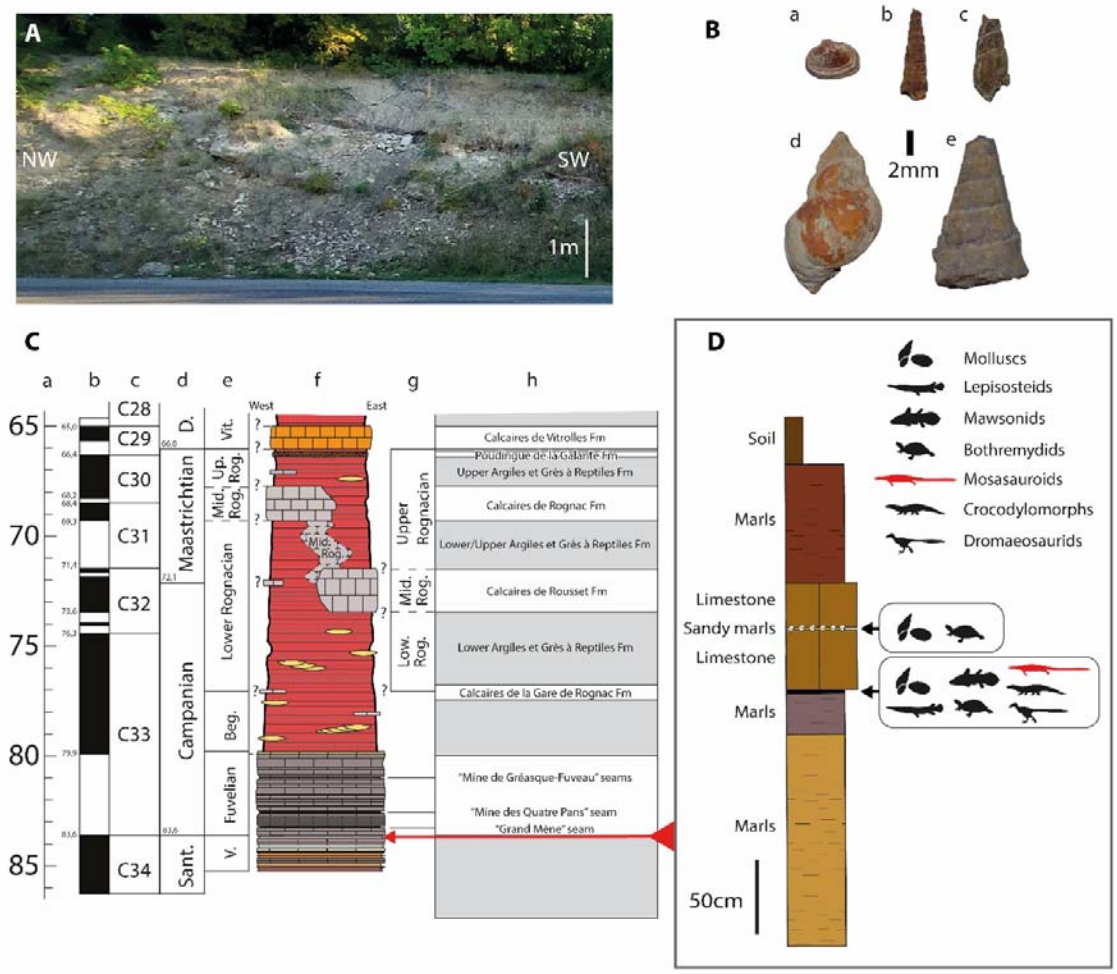

Figure 2 - Stratigraphical details of the Bouc-Bel-Air - Sousquières (BBAS) outcrop. **A**, Photograph of the site where *Garamaudo* was unearthed. **B**, molluscan assemblage found at BBSA, with *Corbicula concinna* (B-a), *Hadraxon acicula* (B-b), "*Melania vasseuri*" (B-c), *Viviparus bosquiana* (B-d) and *Melania colloti* (B-e). **C**, stratigraphical position of BBAS in time scale with standard ages (C-a), geomagnetic polarity (C-b), chronozones (C-c), marine stratigraphy (C-d) and local continental facies (C-e, C-g), synthetic log of the Upper Cretaceous continental deposits of Aix-en-Provence Basin (C-f) with main continental formations (C-h), modified from Cojan & Moreau (2006), Gradstein *et al.* (2020) and Tortosa & Leleu (2021). **D**, detailed log and fossil-bearing horizons.

Direct correlations with the well-documented Valdonnian–Fuvelian succession of the Gardanne coal Basin (Caillol *et al*., 1988; Gonzalez, 1990) remain difficult because of the local tectonic context. The site lies on a structural slice bounded to the north by the Gardanne unit (limited by the Safre Fault) and to the south by the Simiane–Mimet and Sousquières thrust sheets (Guieu, 1968). The section described by Honoré (1938) at La Malle is lithologically similar to that of BBAS, and their fossil assemblages are directly comparable (Honoré, 1938; Fabre-Taxy, 1951). The absence of massive Fuvelian limestones in the immediate surroundings suggests either a rapid lateral facies variation toward more marly deposits, or a slightly older stratigraphic position corresponding to the transition between the Valdonnian and Fuvelian units (Dufaure *et al*., 1967; Babinot &

Durand, 1980). The presence of *Melania colloti*, together with the tectonic compressions observed along the southern margin of the Gardanne Basin, support the latter hypothesis (Durand & Guieu, 1980). Pending further geological investigations, the BBAS locality is here interpreted as lying within the transition between the upper marly Valdonnian facies and the lower calcareous Fuvelian facies, in agreement with previous preliminary work on this locality (Cavin *et al*., 2020). This interval corresponds to a major episode of continental carbonate sedimentation, coeval with the progressive emergence of Provence and the establishment of an extensive endorheic lacustrine system in the Aix-en-Provence basin (Durand & Guieu, 1980; Tortosa & Leleu, 2021).

Magnetostratigraphic studies suggest a Santonian age for the site (Westphal & Durand, 1990; corrected from Cojan & Moreau, 2006) (Figure 2C), making it one of the oldest Upper Cretaceous continental vertebrate localities of southeastern France, along with Ventabren – Air de Repos (Cavin *et al.*, 2020) and Belcodène – Autoroute Diffuseur (Tortosa, 2014).

Material and methods

Material

The material consists of at least two specimens: the first one (Specimen 1) is composed of about twenty remains (CD13-PAL.2018.3.1.1-16, .18), including cranial, axial and appendicular elements, found in close association during one excavation campaign underwent by the Muséum d'Histoire Naturelle of Aix-en-Provence (MHNA) in 1997. The second one (Specimen 2) is a vertebra (CD13-PAL.2018.3.4), coming from the same stratigraphical level but about 20 meters away from the main outcrop, recovered during a rescue campaign in 2018; it is referred to the same taxon. Some vertebral fragments (CD13-PAL.2018.3.1.17, CD13-PAL.2018.3.2, CD13-PAL.2018.3.3) were recovered with Specimen 1 but they remain too incomplete to be safely referred to it.

Comparative Anatomy

Bone comparisons have been made the existing literature for extinct squamates (mosasauroids, ophidiomorphs) and extant *Varanus* skeletons from the MNHN Comparative Anatomy Collections (MNHN AC 1910-12, MNHN AC 1983-6).

The original position of the vertebrae along the vertebral column was assumed based on comparisons with modern varanids and fossil pythonomorphs Cope, 1869 (*sensu* Lee, 1997).

CT-scanning

Three vertebrae (CD13-PAL.2018.3.1.1, CD13-PAL.2018.3.1.3, CD13-PAL.2018.3.4), one rib (CD13-PAL.2018.3.1.13) and the humerus (CD13-PAL.2018.3.1.16), belonging to specimens 1 and 2, were scanned using high-resolution computed tomography at the MRI platform, hosted at the ISEM, University of Montpellier (UMR 5554; EasyTom 40-150, RX Solutions), with reconstructions performed using X-Act (RX Solutions). Voxel size naturally varies pending on specimen size: 17.8 µm

(humerus and vertebra CD13-PAL.2018.3.4), 23.1 µm (vertebra CD13-PAL.2018.3.1.1), 21.5 µm (vertebra CD13-PAL.2018.3.1.3) and 24.2 (rib).

Image segmentation and visualization were performed using VGSTUDIOMAX, version 2.2 (Volume Graphics Inc.). Virtual sections were made in the mid-sagittal and neutral transverse planes for the vertebrae, i.e., the two reference planes for vertebral sections (see Buffrénil et al., 2008) and slightly away from this plane for the CD13-PAL.2018.3.4 sagittal section, for preservation reasons, on the coronal and sagittal planes for the humerus, and in the sagittalplane as well as in two transverse planes (proximally and at about one third of its length) for the rib.

Phylogenetic analysis

To understand the phylogenetical affinities of the new here described genus within Mosasauroidea (*sensu* Augusta *et al.*, 2022), we use the matrix of Zietlow *et al.* (2023), which is a modified version of Strong *et al.* (2020), itself adapted from the pioneer matrix of Bell (1997).

Conversely to Simões *et al.* (2017) and Strong *et al.* (2020) who choose as outgroup for mosasauroids only ophidiomorphs and “aigialosaurids”, both taxa frequently considered the closest relatives and part of Mosasauroidea respectively (e.g. Bell 1997; Zietlow et al., 2023), we follow Polcyn et al (2022) and Zietlow *et al.* (2023) and include as outgroup four Varanoidea, one Shinisauridae, three ophidiomorphs (Appendix 1) but exclude *Ovoo gurvel* due to its incompleteness.

Our ingroup consists of 55 mosasauroid species, that correspond to the here described new genus, the Villeveyrac mosasauroid, which is the second most complete taxon coming from almost coeval freshwater deposits of Southern France (Garcia *et al.*, 2015), as well as six basal mosasauroids (“aigialosaurids”), three halisaurines, twenty-three mosasaurines, eleven plioplatecarpines, five tylosaurines, three yaguarasaurines and two tethysaurines, scored based on their descriptions and on coding provided by Mekarski (2017) (Appendix 1).

The analysis was performed using PAUP version 4.0a169 (Swofford 2003). According to Gauthier *et al.* (2012), multistate characters involving quantitative variation are ordered. Therefore, we designated characters 8, 19, 20, 23, 27, 29, 32, 36, 37, 41, 50, 52, 60, 75, 76, 79, 82, 83, 85, 86, 87, 89, 92, 93, 94, 100, 111, 118, 125 and 127 as ordered in our analysis. Five characters were added and one was modified (see Appendix 1). All characters were unweighted. We modified the scores for fifteen taxa, especially *Pannoniasaurus* and *Tethysaurus*, based on literature and personal observations.

The new data matrix (Appendix 2) was analysed using heuristic search algorithms. The apomorphy list was interpreted using the accelerated transformation (ACCTRAN) setting. Because three ophidiomorph taxa were included as external terminals, we rooted the analysis using a paraphyletic outgroup series to provide broader sampling of putative plesiomorphic character states. Bootstrap support values were calculated and are statistically correlated with Bremer indices (e.g., bootstrap <50% corresponds to Bremer indices of 0–2), while jackknife values, also computed, are particularly informative for morphological datasets (Darlu et al., 2019). To assess data completeness and its potential impact on the resolution and robustness of the phylogenetic analyses, the percentage of missing data was calculated for each taxon (Appendix 1).

The phylogeny obtained was time-scaled (Figure 10), using the R package Strap (Bell & Lloyd, 2015), running into the software R version 4.3.0 (2023). First appearance datum (FAD) and last appearance datum (LAD) of each taxon were taken from the Paleobiology Database (http://paleobiodb.org/), with the exception of the Santonian here described mosasauroid, constrained (FAD = 84 Ma, LAD = 83.6 Ma) by magnetostratigraphical analyses (see Westphal & Durand, 1990) and the early Campanian Villeveyrac mosasauroid, constrained (FAD = 83.6, LAD = 80 Ma) on biostratigraphical evidence (see Garcia et al., 2015).

Abbreviations: CD13 - Conseil départemental des Bouches-du-Rhône, Marseille, France; MHNA - Muséum d'Histoire Naturelle d'Aix-en-Provence, Aix-en-Provence, France; MNHN - Muséum National d'Histoire Naturelle, Paris, France.

Systematic Palaeontology

Reptilia Laurenti, 1768
Squamata Oppel, 1811
Mosasauridae Gervais, 1852
Tethysaurinae Makádi *et al.*, 2012

***Garamaudo bauciensis* nov. gen., nov. sp.**

Etymology – From "*Gara au maudo*", a Provençal expression meaning "beware the cursed one", referring to a malevolent serpentiform creature, the Garamaudo, said to haunt local freshwaters, and first mentioned by Frédéric Mistral in *Mirèio* (1859). The specific epithet *bauciensis* means "from Bouc-Bel-Air", the type locality.

Holotype – CD13-PAL.2018.3.1.1-16,18 (Figures 3-7), an incomplete skeleton (called "Specimen 1") found in 1997, including the incomplete posterior part of the left mandible (CD13-PAL.2018.3.1.10), nine vertebrae including five cervicals (CD13-PAL.2018.3.1.1, .3, .5, .7, .8), one dorsal (CD13-PAL.2018.3.1.4), two indeterminate ones (CD13-PAL.2018.3.1.2, .6), six ribs (CD13-PAL.2018.3.1.9, .12, .13, .14, .15, .18), a right humerus (CD13-PAL.2018.3.1.16), and a right incomplete pelvis (CD13-PAL.2018.3.11).

Referred specimens – CD13-PAL.2018.3.4 (Figure 7G-I, 8E), a dorsal vertebra (called "Specimen 2") found in 2018 in the same outcrop and level than "Specimen 1", but about twenty meters from the *locus typicus*.

Geographical and stratigraphical occurrences – Bouc-Bel-Air - Sousquière outcrop (BBAS), near Aix-en-Provence, Bouches-du-Rhône Department, Provence, southeastern France; Level 99, Valdonnian local facies, Santonian (Durand & Guieu, 1980).

Diagnosis – Autapomorphies: Posterior mandibular unit (PMU) strongly curved inward in dorsal/ventral view; Surangular with a medial horizontal triangular plateau located just anteriorly to the anterior border of the glenoid fossa; Retroarticular process oriented obliquely about 45° to the long axis of the PMU, extremely short (half the length of the glenoid fossa), with a regularly convex half-moon posterior margin prolonged antero-medially by an anteriorly oriented hook; A*dductor fossa* of the surangular opened along its length, being located dorsally and parallel to the surangular/prearticular-articular suture; Ribcage high dorsoventrally and laterally compressed, composed of very elongated and straight ribs, being only curved at the proximal third of their length at an angle of about 35°; Humerus, though long and slender, being much smaller than the PMU, indicating a possibly reduced anterior limb; Pubis with a very long and slender anterior process, oriented in the body longitudinal axis.
Plesiomorphies retained by *Garamaudo*: PMU being long, slender and rectangular with glenoid fossa made mainly by the articular; humerus long and straight with epiphyses almost perpendicularly oriented one to each other; pubis with ilium, ischium and pubis firmly fused at the level of the oval acetabulum and ilium posteriorly oriented.

Description

General preservation

Most bones (posterior mandibular unit, most vertebrae, ribs, pelvis) are of similar size, without any repetition, and have been found in close association during the same field campaign (1997), suggesting that they probably belong to the same individual, called “Specimen 1”. However, it should be pointed out that one dorsal vertebra (CD13-PAL.2018.3.1.4) and the humerus (CD13-PAL.2018.3.1.16) differ in size from the rest of the material: the vertebra is comparatively much larger and the humerus much smaller. Also, one dorsal vertebra (CD13-PAL.2018.3.4) – called “Specimen 2” - has been found a decade later (2018) about twenty meters from the main outcrop; it is of comparable size than most of the material and is referred to the same taxon. The microanatomical features of the various bones analyzed are consistent, whatever their size and occurrence, supporting that they probably belong to the same taxon, although to at least two different individuals.

The bones are generally not well preserved, especially the vertebrae (none is complete), exhibiting several alterations such as lateral or dorsal compressions, breakages, as well as frequent abrasion, perforation and/or selachian predation/scavenging marks (NB pers. obs.) on their external surface. Conversely, some bones remain relatively complete (posterior mandibular unit, pelvis) and their external surface relatively well preserved. As a whole, the state of preservation of the bones indicates that the transport could have been short after the death of the more complete specimen (“Specimen 1”) and before its burial (explaining that some bones remain relatively complete and not abraded), but that it occurred in a rather high energy episode, maybe a flooding (explaining why the skeleton is disarticulated and some bones broken), which is in agreement with the paleoenvironement proposed, that is a freshwater lake periodically influenced by flooding and shallowing events (see Discussion). In addition,

the occurrence of at least two individuals belonging to the same taxon also suggests that this basal mosasaurid was possibly autochthonous or sub-autochthonous to this freshwater environment, as already observed in several Late Cretaceous continental outcrops from Europe (see Introduction and Discussion).

Cranial skeleton

The only cranial element (CD13-PAL.2018.3.1.10) preserved is the left posterior mandibular unit (abbreviated as PMU from now on) of which the almost complete surangular and prearticular-articular, and a very small part of the angular, are preserved (Figure 3). The coronoid, which is usually loosely “saddled” above the surangular and prearticular, lacks.

The **PMU** has the shape of a long and low rectangle in lateral/medial views (length about 12.8 cm, median height about 2.3 cm) (Figure 3A-D) and is curved inward in dorsal/ventral view (Figure 3E-H). Its ventral margin is slightly sigmoid in lateral/medial view, being convex anteriorly, concave in its median part, then convex again posteriorly (Figure 3A-D). The concave median part is usually occupied by the angular (see below), which, when preserved, gives the ventral margin of the PMU a straighter aspect.

The **surangular** is an elongated and low rectangular bone (length about 11.8 cm) that occupies most of the lateral surface of the PMU (Figure 3A-B), except its posterior part occupied by the articular. Its anterior portion, though not well preserved, appears slightly oblique dorso-ventrally. The lateral surface of the bone is gently convex dorso-ventrally and bears a marked longitudinal straight ridge (for attachment of the *pseudotemporalis superficialis* and *adductor mandibulae* muscles), located slightly above the mid-height of the bone and rising slightly forward. Anteriorly, this ridge is bordered ventrally by a shallow groove; posteriorly it is rugose and bordered by an oval concavity and an oval foramen, nestled in a shallow groove that ends up just ventrally to the anterior margin of the glenoid fossa. Ventrally to this posterior part of the ridge, the surangular is very rugose. The ventral suture of the surangular with the prearticular-articular is straight and located on the ventral margin of the mandible so that the prearticular-articular is poorly visible in lateral view (Figure 3A-B). Posteriorly, this suture curves abruptly dorsally with an angle of about 50° up to the posterolateral corner of the glenoid fossa, ending into a sharp laterally oriented corner. From this corner, the surangular rises in a straight line anteriorly for most of its dorsal margin length, before curving abruptly concavely where the coronoid articulates. In dorsal view, from the antero-lateral sharp corner of the glenoid fossa, the surangular curves perpendicularly medially into a sigmoid elevated dorsal lip, that makes the anterior border of the glenoid fossa, and its only participation into it (Figure 3E-F). This lip carries on anteriorly on the medial surface of the bone by a unique concave triangular plateau roughly horizontally oriented (Figure 3E-F), then the bone becomes vertical along its length. In medial view, the suture with the prearticular-articular is concave from the anterior border of the glenoid fossa, then runs horizontal along most of its length before sloping dorsally in its anterior part (Figure 3C-D). This suture is poorly visible and is located on the first third of the height of the PMU, meaning that the surangular participation in its medial surface is much larger than that of the prearticular-articular. The shallow *adductor fossa* is located dorsally and parallel to the surangular/prearticular-articular suture. It is unique in being opened (i.e. not covered anteriorly by a thin descending blade of bone) and, as such, it

extends for most of the length of the surangular. The region where the mandibular foramen should have occurred is broken. Antero-dorsally, the suture for the coronoid is long, occupying about 1/3 of the PMU length, and narrow, showing that the medial coronoid wing should not be very extended ventrally; the coronoid buttress is also poorly developed (Figure 3C-D).

The **angular** is possibly represented by two tiny thin blades of bone located between the surangular and the prearticular-articular: one anteriorly, about 2.5 cm long, visible on medial view; the other visible laterally around the middle ventral surface of the PMU (Figure 3A-D). The ventral surface of the PMU bears a shallow slender longitudinal groove for the articulation of the angular that extends very far posteriorly (to about ¾ of its total PMU length) where it tapers in a sharp thin extremity (Figure 3G-H). It is medial anteriorly, then passes lateral posteriorly.

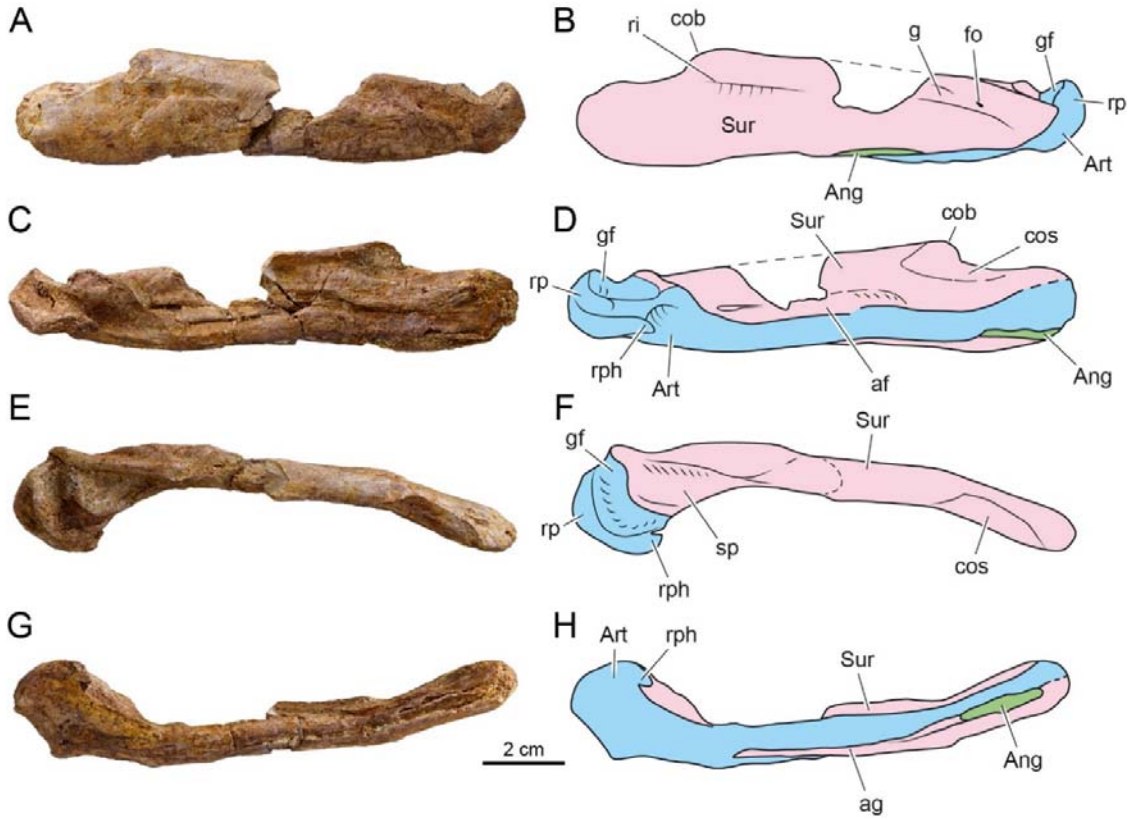

Figure 3 - *Garamaudo bauciensis* nov. gen., nov. sp., mandible. Holotype (CD13-PAL.2018.3.1.10), Bouc-Bel-Air - Sousquière (Bouches-du-Rhône Department, Provence, southeastern France), Santonian. **A-H**, photographies and interpretative drawings in lateral (**A-B**), medial (**C-D**), dorsal (**E-F**) and ventral (**G-H**) views. **Abbreviations**: af, *adductor fossa*; Ang, Angular; angg, angular groove; Art, Prearticular-articular unit; cos, coronoid suture; cob, coronoid buttress; fo, foramen; g, groove; gf, glenoid fossa; ri, ridge; rp, retroarticular process; rph, retroarticular process hook; sp, Sur, surangular; sp, surangular horizontal plateau.

The **prearticular** and **articular** are fused into a single bone without any visible suture, as usually in mosasaurids (Russell, 1967). The unit occupies all the length of the PMU (that is 12.8 cm) and half of its medial surface (Figure 3C-D), but remains poorly

visible in lateral view (Figure 3A-D). In medial view, the prearticular-articular is a horizontal slender bone that expands posteriorly at the level of the glenoid fossa and retroarticular process. The glenoid articulation is plesiomorphic, made mainly by the articular, the surangular participating only in its anterior margin; it is slightly concave, transversally oriented, about twice wider than long and reniform in shape, with a sigmoid anterior margin and a concave posterior one (Figure 3C-F). Both anterior and posterior margins are elevated rugose “lips”, whereas the lateral and medial margins are flat, suggesting that the quadrate sliding movement for the opening of the jaws was mainly dorso-ventral. The retroarticular process is oriented obliquely at about 45° to the long axis of the PMU and bears a fan shape appearance (Figure 3E-H). It is unique in being extremely short, being 1/2 of the glenoid fossa length, and in bearing a regularly convex half-moon shaped posterior margin, prolonged antero-medially by an anteriorly oriented hook, creating a medial fossa ventrally to the glenoid fossa (Figure 3C-F). The retroarticular process bears a large oval foramen located just ventral to the medio-posterior corner of the glenoid fossa.

Axial skeleton

The axial skeleton includes several vertebrae including five cervicals (CD13-PAL.2018.3.1.1, .3, .5, .6, .7, .8), two dorsals (CD13-PAL.2018.3.1.4, CD13-PAL.2018.3.4), and one indeterminate one (CD13-PAL.2018.3.1.2), as well as six ribs (CD13-PAL.2018.3.1.9, .12, .13-15, .18).

Vertebrae

All vertebrae are procoelous and do not display pachyostosis (Figure 4). Based on the broken parts available, it appears that prezygapophyses are rather strongly projected anteriorly, extending well beyond the anterior border of the cotyle (Figure 4C, G).

Cervical vertebrae

CD13-PAL.2018.3.1.3 consists in two partial anterior cervical vertebrae articulated: part of the atlas and the axis (Figure 4A-B). The axis shows a long hypapophyseal peduncle, strongly projecting ventrally, with an ovoid facet antero-posteriorly directed and almost horizontal, that is ventrally oriented. Anteriorly, the axis intercentrum articulates ventrally with both the anteriormost part of the centrum, through an antero-ventral facet, but also to the atlas, through a postero-ventral facet. It seems to end in a small ovoid antero-posteriorly elongated facet pointing ventrally and slightly posteriorly. Paradiapophyses are very short dorso-ventrally and very posteriorly located, with marked dorsal and ventral ridges. The neural canal is much thinner than the condyle.

CD13-PAL.2018.3.1.1 is an anterior cervical vertebra (Figure 4C-E), as shown by the well-developed hypapophyseal peduncle, continuous with the centrum that ends, below the condyle, in an ovoid concave facet dorso-ventrally elongated and oriented very posteriorly and ventrally (Figure 4C-D). The hypapophysis is not fused. The centrum is elongated. The condyle is much ovoid (Figure 4E), being medio-laterally extended (dorso-ventrally compressed) and there is no precondylar constriction. The cotyle-condyle axis is horizontal. The paradiapophyseal facet is dorso-ventrally rather short and appears projected much posteriorly and a marked anterodorsal diapophyseal ridge links its dorsal border to the prezygapophysis. The ventral parapophyseal lamina (prolonging

antero-ventrally the paradiapophyses; see Houssaye *et al.*, 2011) anteriorly extends much ventrally, way beyond the ventral border of the cotyle. The preserved postzygapophysis has a large facet latero-ventrally directed (Figure 4E). The posterior view suggests the occurrence of a zygantrum, although no zygantral facet is visible, apparently with zygosphenal foramina. The neural canal appears rather cylindrical, with a flattened ventral border and a trilobate aspect formed by the two ‘‘ridges’’ running along the lateral walls, and much thinner and lower than the condyle (Figure 4E). The neural spine raises from about a third of the centrum length and appears rather short with a horizontal roof, and does not extend beyond the condyle (Figure 4C).

CD13-PAL.2018.3.1.8 is a broken rather anterior cervical vertebra as shown by the probably ventral extension of the paradiapophyses and the hypapophyseal peduncle with a facet facing probably much posteriorly.

CD13-PAL.2018.3.1.6 and **CD13-PAL.2018.3.1.7** are parts of the same broken vertebra. It is a more posterior cervical vertebra with a higher cotyle, probably more circular. The paradiapophyses extend slightly below the centrum and are much more extended dorso-ventrally. The posterior part of the centrum is nor preserved, preventing the possibility to state on the possible occurrence and shape of a hypapophyseal peduncle.

CD13-PAL.2018.3.1.5 consists in articulated very partial cervical vertebrae with paradiapophyses projecting much beyond the ventral border of the centrum and a prezygapophysis projecting much anteriorly.

Dorsal vertebrae

CD13-PAL.2018.3.4 is a rather anterior dorsal vertebra (Figure 4G-I). The paradiapophyses do not extend below the ventral border of the centrum (Figure 4H) and are very anteriorly located; they are subvertical and extend up to the base of the prezygapophyses (Figure 4G). The epidiapophyseal ridge and the lateral border of the centrum ventrally are well marked. In dorsal view, the narrowest part of the interzygapophyseal constriction appears rather posterior. The centrum is relatively shorter than in CD13-PAL.2018.3.1.4. and more triangular. The posterior border of the neural arch is concave and the arch is thick (Figure 4I), while the neural spine appears rather short. It raises from below the paradiapophyses, is shorter than in CD13-PAL.2018.3.1.1., and does not extend beyond the condyle. The cotyle-condyle axis straightness or obliquity cannot be determined. One zygantral foramen is visible.

CD13-PAL.2018.3.1.4 is a large elongated vertebra with an ovoid condyle, dorso-ventrally compressed. Its long and flat centrum is reminiscent of posterior dorsals (Figure 4F).

There is a rather high difference in centrum length between the two dorsal vertebrae CD13-PAL.2018.3.4 (about 2.5 cm) and CD13-PAL.2018.3.1.4. (estimated about 4.7 cm) suggesting that at least two specimens are present in the deposit.

Indeterminate vertebrae

CD13-PAL.2018.3.1.2 is extremely partial and only shows that prezygapophyses are oriented antero-laterally and an ovoid cotyle.

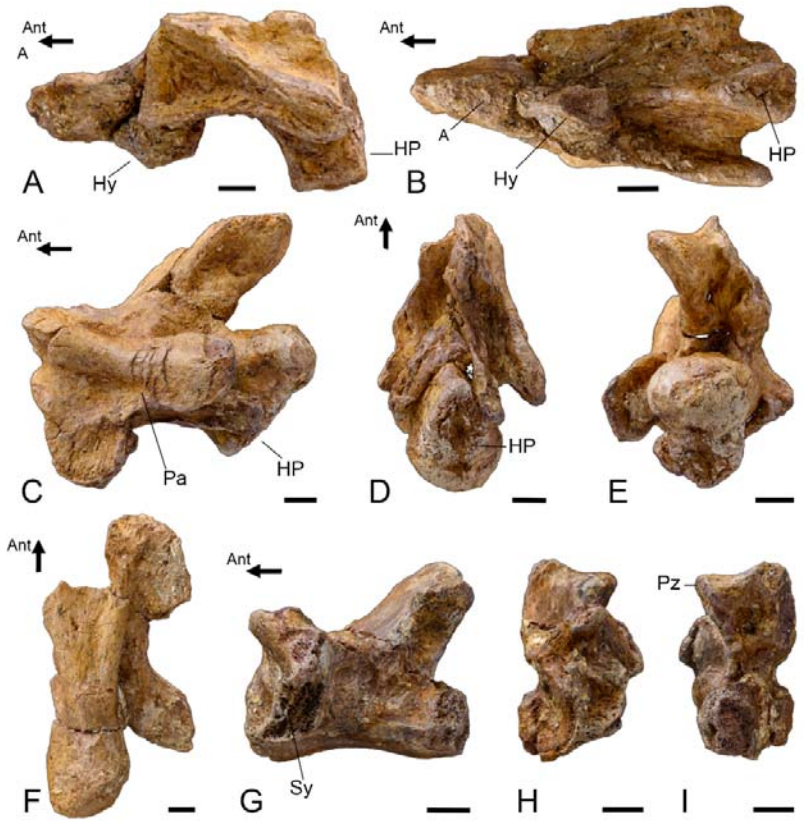

Figure 4 - *Garamaudo bauciensis* nov. gen., nov. sp., vertebrae. Holotype (CD13-PAL.2018.3.1.1, .3, .4) and referred specimen (CD13-PAL.2018.3.4), Bouc-Bel-Air - Sousquière (Bouches-du-Rhône Department, Provence, southeastern France), Santonian. **A-B**, CD13-PAL.2018.3.1.3, Axis with part of the atlas in right lateral (**A**, mirrored) and ventral (**B**) views. **C-E**, CD13-PAL.2018.3.1.1, anterior cervical vertebra in left lateral (**C**), ventral (**D**) and posterior (**E**) views. **F**, CD13-PAL.2018.3.1.4, dorsal vertebra in ventral view. **G-I**, CD13-PAL.2018.3.4, dorsal vertebra in left lateral (**G**), anterior (**H**) and posterior (**I**) views. **Abbreviations**: A, atlas; Ant, anterior direction; Cd, condyle; Ct, cotyle; Dr, diapophyseal ridge; Er, epidiapophyseal ridge; HP, hypapophyseal peduncle; Hy, hypapophysis; Pa, paradiapophysis; Pl, parapophyseal lamina; Pz, postzygapophysis. Scale bars = 5 mm.

Ribs

Six ribs are preserved, of which two are almost entirely preserved. They are very elongated and straight, being only curved at the proximal third of their length at an angle of about 35° (Figure 5). As a consequence, the ribcage was not extended laterally but rather high dorsoventrally and laterally compressed. If there seems to be a single articulation, the ovoid, medio-laterally compressed, head is slightly double-headed, due to a small posterior peduncle.

CD13-PAL.2018.3.1.9 is a sternal rib. It shows the fusioned intermediate portion, after the dorsal intercostal joint, up to the ventral intercostal joint. This part is curved medially.

CD1 3-PAL.2018.3.1.13 is a more posterior rib. It is longer (about 15 cm in a straight line [15.2 along its curve] from the most proximal to the most distal point preserved versus the less than 11 cm [11.5 along its curve] up to the dorsal intercostal joint – about 13.8 [16 along the curve] up to the ventral one of CD13-PAL.2018.3.1.9).

Other proximal portions of ribs show a consistent morphology.

Figure 5. *Garamaudo bauciensis* nov. gen., nov. sp., ribs. Holotype (CD13-PAL.2018.3.1.9, .13), Bouc-Bel-Air - Sousquière (Bouches-du-Rhône Department, Provence, Southeastern France), Santonian. **A**, CD13-PAL.2018.3.1.9, sternal rib; **B**, CD13-PAL.2018.3.1.13, posterior rib. **Abbreviations**: dij, dorsal intercostal joint; ip, intermediate portion; pp, posterior peduncle.

Appendicular skeleton

The appendicular skeleton is represented by a right humerus and an incomplete right hemi-pelvis.

Anterior limb

The **humerus** (CD13-PAL.2018.3.1.16) is long (preserved length about 7 cm), straight and slender, with a long diaphysis about 1/3 of the total length (Figure 6A-H), and proximal and distal extremities almost perpendicularly oriented one to each other (Figure 6I-J). The diaphysis is slightly flattened dorso-ventrally with its median part stout (about 1 cm wide) and roughly rounded in cross-section. The proximal articular surface is oval, about 1.9 cm width, rugose, and slightly posteriorly deflected from the longitudinal axis of the diaphysis. The deltopectoral crest is a thin blade of bone, developed on the third upper proximal third of the bone (Figure 6C-F); it is not separated from the proximal articular head by a deep groove like in *Varanus* and is oriented about 115° from it, leaving a shallow concave triangular area between both structures (Figure 6C-D). The dorsal surface of the humerus is strongly convex and bears a sharp longitudinal ridge running from the posterior corner of the proximal articulation surface to the posterior ectepicondyle zone (Figure 6A-B). The distal epiphysis is broken, but the fragmentary entepicondyle and ectepicondyle show that is what probably enlarged. A small tubercle is preserved on the upper postero-distal third of the bone (Figure 6E-F), reminiscent of the one present in *Varanus* and basal mosasauroids (DeBraga & Carroll, 1993). Though being long and slender, the humerus is astonishingly much smaller than the PMU - in extant varanids and in plesiopedal mosasaurids it is about the same size (NB, pers. obs).

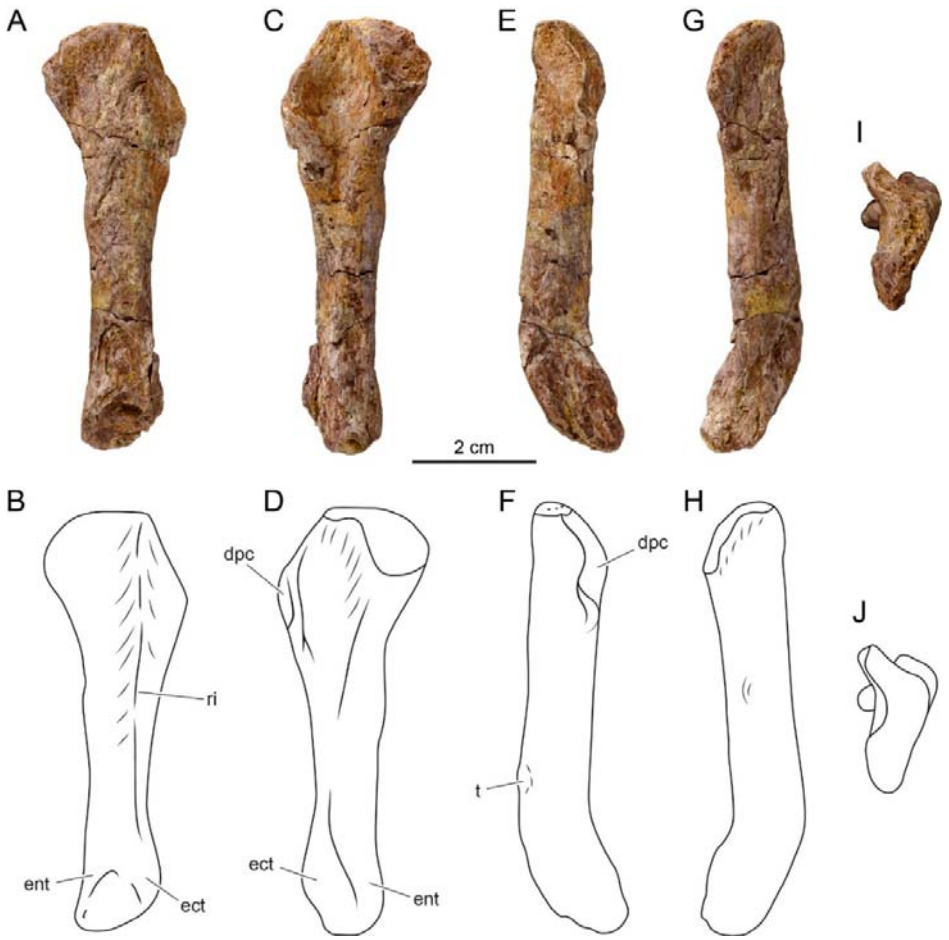

Figure 6.

***Garamaudo bauciensis* nov. gen., nov. sp., humerus.** Holotype (CD13-PAL.2018.3.1.16), Bouc-Bel-Air - Sousquière (Bouches-du-Rhône Department, Provence, Southeastern France), Santonian. **A-J**, photographies and interpretative drawings in dorsal (**A-B**), ventral (**C-D**), anterior (**E-F**), posterior (**G-H**) and proximal (**I-J**) views. **Abbreviations**: ect, ectepicondyle; ent, entepicondyle; dpc, deltopectoral crest; ri, ridge; t, tubercle.

Pelvis girdle

The **pelvis** (CD13-PAL.2018.3.11) is about 14 cm long, being coherent in size with the posterior mandibular unit and most vertebrae (NB, pers. obs.) so that it is assumed it belongs to Specimen 1. It includes the almost complete ilium and pubis and only the acetabular portion of the ischium (Figure 7). The three bones are firmly fused together at the level of the acetabulum, which is deeply concave and roughly oval. The suture between the three bones is clearly still visible on both lateral and medial views (Figure 7A-D).

The **ilium** is about 8 cm long but its posterior extremity lacks, so that it could have been about the same length as the pubis. It is a robust rod of bone postero-dorsally oriented. Its participation in the acetabulum is the largest of the three pelvic bones, forming all its dorsal portion (Figure 7A-B). Its ventral articulations with both the pubis anteriorly and the ischium posteriorly are obliquely oriented to each other at about 120°, having as such an open V shape (Figure 7A-B). The anterior preacetabular process is a small rounded tongue of bone, laterally compressed and anteriorly oriented, slightly

protruding over the pubis articulation. Ventro-posteriorly, the ilium butts up against the ischium in a reinforced rounded portion.

The **pubis** is about 8.3 cm long and almost flat. It participates into the antero-ventral part of the acetabulum into an oblique long suture with the ilium and a shorter vertical one with the ischium (Figure 7A-D). The proximal part of the pubis is expanded, with a large rectangular pubic tubercle, mostly dorsally and only slightly laterally oriented (Figure XA-D) and a large and oval obturator foramen laying roughly in the median part of the bone in medial view, but being displaced more ventrally in lateral view (Figure 7A-D). The anterior process of the pubis is unique in being very long and slender, triangular in section and notably oriented in the same plan than the body longitudinal axis and not perpendicular to it (Figure 7E-F). In lateral view this anterior process is regularly curved from the horizontal, forming a bowed structure ending in a vertical tip. Also in lateral view, its dorsal surface is sigmoid, being strongly concave anterior to the pubic tubercle, then convex, finally straight, whereas its ventral surface is regularly concave along its length.

The **ischium** is represented only by its acetabular part, having a long and oblique suture with the ilium and a vertical shorter one with the pubis (Figure 7A-D). It is not possible to determinate if, like the pubis, it laid in the same axis than the ilium and pubis or was internally oriented to meet its opposite in a median suture (e.g. DeBraga & Carroll, 1993).

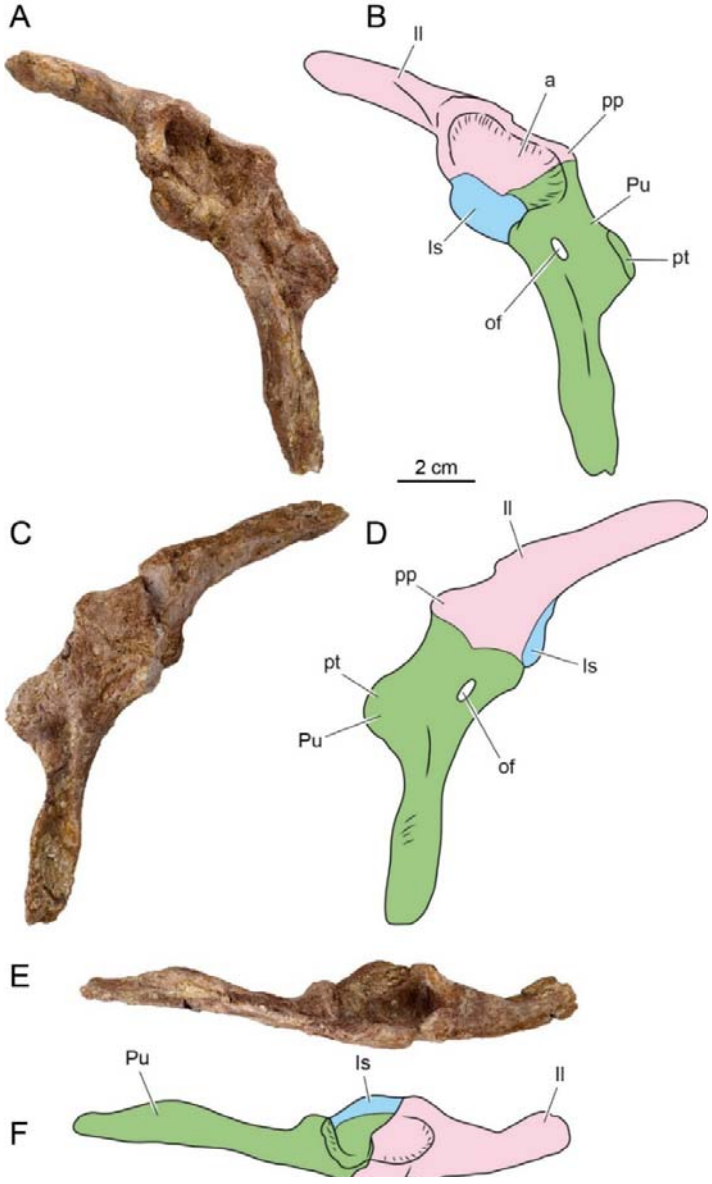

Figure 7. *Garamaudo bauciensis* nov. gen., nov. sp., pelvic girdle. Holotype (CD13-PAL.2018.3.1.11), Bouc-Bel-Air - Sousquière (Bouches-du-Rhône Department, Provence, Southeastern France), Santonian. **A-F**, photographies and interpretative drawings in lateral (**A-B**), medial (**C-D**) and dorsal (**E-F**) views. **Abbreviations**: a, acetabulum; Il, Ilium; Is, Ischium; of, obturator foramen; pp, preacetabular process; Pu, Pubis; pt, pubic tubercle.

Microanatomy

The vertebrae show a relatively thick layer of compact cortex, a bit thicker in the axis (Figure 8A) than in the anterior cervical and dorsal vertebrae (Figure 8C), and a high inner compactness, as compared to modern lizards, far from their typical tubular inner organization, with one outer layer of compact bone surrounding the bone and another surrounding the neural canal and a few trabeculae connecting them (Houssaye *et al.*, 2010). Even the endochondral territory shows only small cavities. However, larger cavities linked to active resorption are observable in the periosteal territory. The hypapophyseal peduncle is less compact than the rest of the vertebra. Some simple vascular canals radially oriented are observed in the cortex in transverse sections, notably in CD13-PAL.2018.3.4 (Figure 8B, D, E; much less visible in the longitudinal ones).

The rib shows a thick cortex surrounding a compact spongiosa and no open medullary cavity (Figure 8F-H). There is a strong asymmetry with a much thicker cortex dorsally (Figure 8F). The thickness increases progressively from the proximal part to about the third of the rib length and then progressively decreases.

Figure 8. *Garamaudo bauciensis* nov. gen., nov. sp., vertebral and rib microanatomy. Holotype (CD13-PAL.2018.3.1.1, .3) and refered specimen (CD13-PAL.2018.3.4), Bouc-Bel-Air - Sousquière (Bouches-du-Rhône Department, Provence, Southeastern France), Santonian. **A-E**, Vertebral virtual sections of CD13-PAL.2018.3.1.3 (**A-B**), CD13-PAL.2018.3.1.1 (**C-D**), CD13-PAL.2018.3.4 (**E**), in mid-sagittal (**A, C**) and transverse (near the growth center; **B, D, E**) sections. **F-H**, Rib CD13-PAL.2018.3.1.13 longitudinal (**F**) and transverse (**G-H**; see sectional planes on **G**) sections. Scale bars = 5mm (**A-F**) and 2 mm (**G-H**).

The humerus longitudinal sections show a clear hourglass-shape in the compact cortex distribution, with a maximal compactness at the growth center, which appears close to the mid-diaphysis (Figure 8A-C). There seems to be a small medullary cavity in the core of the diaphysis and the rest of the medullary area is filled by a spongiosa whose tightness decreases toward the core of the bone. As a consequence, the bone is strongly compact. Primary cortical bone clearly displays growth marks and some radial simple vascular canals are observed.

As a whole the vertebrae, rib and humerus of *Garamaudo bauciensis* clearly show, by comparison with modern squamates (Houssaye *et al.*, 2010), osteosclerosis, with an inhibition of primary bone resorption, as shown by the relatively high thickness of primary

compact cortex. The primary nature of these deposits is clearly indicated by the growth marks and vascularization when visible.

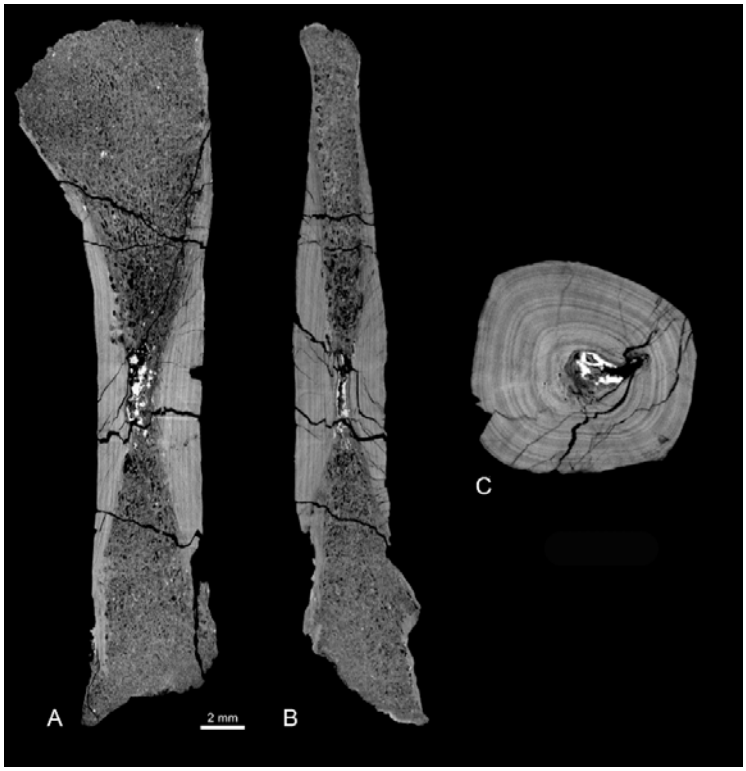

Figure 9. *Garamaudo bauciensis* nov. gen., nov. sp., humerus microanatomy. Holotype (CD13-PAL.2018.3.1.16), Bouc-Bel-Air - Sousquière (Bouches-du-Rhône Department, Provence, Southeastern France), Santonian. **A-C**, coronal (**A**), sagittal (**B**) sections, and transverse section around the growth center (**C**).

Comparisons and systematical attribution

The posterior mandibular unit (PMU) is typical of squamates but differs greatly from that of snakes (whose surangular and articular/prearticular are fused into a single complex; e.g. Lee 1997) and from ophidiomorphs (whose articular is usually visible in lateral view, sandwiched between the angular and the surangular; e.g. Pierce & Caldwell, 2004). It differs also from that of derived mosasaurids, which is proportionally stouter, shorter and more diamond-shaped in lateral view (Russell, 1967). It is comparable to that of basal mosasauroids - like *Aigialosaurus, Haasiasaurus*, tethysaurines and yaguarasaurines - in having roughly a long and slender rectangular shape, and in possessing a glenoid articulation mainly composed of the articular, the surangular participation being reduced to its anterior lip (DeBraga & Carroll, 1993).

Vertebrae are procoelous, as in most other squamates (Hoffstetter & Gasc, 1968). They display features of Varanoidea *sensu* Lee (1997), i.e. Varanidae, Helodermatidae and Pythonomorpha: a hypapophysis of central origin with an articulated distal element, and the posterior position of the narrowest part of the interzygapophyseal constriction. The likely occurrence of a zygantrum suggests that of a zygosphene/zygantrum system was probably present. It characterizes Pythonomorpha Cope, 1869 *sensu* Lee (1997), i.e. Mosasauroidea and Ophidiomorpha *sensu* Palci & Caldwell (2007; i.e. stem Ophidia

[*Adriosaurus*, *Aphanizocnemus*, Dolichosauridae] and Ophidia), that is the clade including the most recent ancestor of mosasaurs, snakes and all its descendants (node-based definition from Caldwell, 2006). The general morphology of the vertebrae is clearly distinct from that of snakes, although the diagnostic characters are not observable on this limited material. It differs also from that of hydropedal mosasauroids and of the plesiopedal and hydropelvic mosasauroid *Dallasaurus* whose centrum is notably more cylindrical and less flat (e.g. Russell, 1967; Bell & Polcyn, 2005). The vertebrae appear very similar to those of freshwater plesiopedal tethysaurines, that are the Villeveyrac taxon from southern France (Garcia et al., 2015) and *Pannoniasaurus* from Hungary (Makádi *et al.*, 2012).

The rib morphology is consistent with that of the stem-Ophidia *Mesoleptos* and of plesiopedal and plesiopelvic mosasauroids (e.g., *Aigialosaurus bucchichi*; *Komensaurus*; Caldwell & Palci, 2007; Dutchak & Caldwell, 2009).

The humerus excludes *de facto* this taxon from snakes. It is clearly plesiopedal, being long and slender, with a long diaphysis making about 1/3 of the total length, and proximal and distal extremities almost perpendicularly oriented one to each other, like in *Varanus*. However, the bone is flatter, shorter and with a stouter rounded epiphysis than in *Varanus*, being reminiscent to plesiopedal mosasauroids, such as *Aigialosaurus* and *Carsosaurus* (DeBraga & Carroll, 1993) or the mosasaurine *Dallasaurus* (Bell & Polcyn, 2005). It differs greatly from the humerus of hydropedal mosasauroids, which is generally very reduced in length compared to its width (Russell, 1967).

The pelvis also excludes this taxon from snakes. The pelvis of the few snakes with a hindlimb, when preserved, is a relatively much smaller triradiate structure, but poorly known and described which limits comparisons (Rieppel *et al.*, 2003; Houssaye *et al.*, 2011; Palci *et al.*, 2013). In possessing three bones firmly fused forming a large oval acetabulum, as well as a posteriorly oriented ilium, it looks like varanids and basal plesiopelvic mosasauroids (“aigialosaurids”, tethysaurines, situation unknown in yaguarasaurines) (DeBraga & Carroll 1993) and strongly differs from hydropelvic mosasaurids where the pelvic bones are unfused and the ilium anteriorly oriented (Russell, 1967). On the contrary however, like hydropelvic mosasaurids, the ilium bears a small and rounded preacetabular process abutting on the pubis, whereas the pubis has a pubic tubercle mostly dorsally oriented, and a long and slender anterior process parallel to the body long axis. In varanids, the ilium preacetabular process is longer and individualized from the main shaft of the bone, the pubis tubercle is rounded and mostly ventro-laterally oriented, and its anterior process, though also long, is oriented perpendicular to the body long axis to meet its opposite in a median suture (DeBraga & Carroll; 1993). In basal mosasauroids, the ilium preacetabular process is also longer, whereas the pubis anterior process is shorter and more fan shaped distally, and appears oriented parallel to the body long axis (e.g. DeBraga & Carroll, 1993). As a whole, the pelvis is unique in exhibiting a mosaic of characters present in both terrestrial varanids, plesiopelvic, and hydropelvic mosasauroids.

As far as the microanatomy is concerned, it permits to differentiate this taxon from several pythonomorphs as follows: 1) The apparent absence of pachyostosis on the vertebrae available differentiate it from most ophidiomorphs that display at least some vertebrae with a bloated aspect (Houssaye, 2013a); 2) The occurrence of osteosclerosis clearly distinguishes this taxon from the other ophidiomorphs (*Dolichosaurus* and

Coniasaurus) that display a “classical” tubular structure (Houssaye, 2013a), from the lizard from Lo Hueco (Houssaye *et al.*, 2013a) that shows compactness values within the range, although among the highest, of modern squamates and a tubular structure in transverse sections, and from hydropedal and hydropelvic mosasauroids with their tight trabecular network (Houssaye & Bardet, 2012). It also distinguishes this taxon from the plesiopedal and plesiopelvic mosasauroid *Tethysaurus* and *Dallasaurus* that displays a rather loose and heterogeneous spongious organization, with a higher density in the periosteal territory, but much less dense than in this taxon (Houssaye, 2008). Similarly, the osteosclerosis in the ribs differs from the much lighter structure observed in the ribs of hydropedal and hydropelvic mosasauroids, the open medullary cavity observed in the ophidiomorph *Kaganaias*, and *Dallasaurus*. It also differs from the more intense osteosclerosis of *Carentonosaurus* (Houssaye, 2013a).

To sum up, both the anatomical and microanatomical characters observed in the cranial, axial and appendicular skeleton of *Garamaudo* permit to refer it to a pythonomorph squamate, and more specifically to a Mosasauroidea (*sensu* Bell & Polcyn, 2005; Caldwell & Palci, 2007).

Garamaudo differs greatly from hydropedal and hydropelvic mosasaurids (*sensu* Bell & Polcyn, 2005; Caldwell & Palci, 2007) that bear: a posterior mandibular unit (PMU) proportionally shorter, deeper and more diamond-shaped in lateral view, centra more cylindrical and less flat, a humerus much shorter and broader, a pelvis with bones unfused and an anteriorly oriented ilium (e.g. Russell, 1967; DeBraga & Carroll, 1993; Zietlow *et al.*, 2023), and a much lighter microanatomical structure made of a tight trabecular network (Houssaye & Bardet, 2012).

It differs also from the basal plesiopedal / hydropelvic mosasaurine *Dallasaurus* that, though exhibiting comparable long and slender humerus, possesses more cylindrical vertebral centra, a slightly shorter humerus with more expanded epiphyses, a pelvis with a loose acetabular articulation and an anteriorly oriented ilium (hydropelvic condition), vertebrae with a much lower compactness, and ribs with an open medullary cavity (Bell & Polcyn, 2005; Houssaye & Bardet, 2012).

Conversely, most of its plesiomorphic characteristics, such as a long and slender PMU, a long and slender humerus with epiphyses almost perpendicularly oriented one to each other, and a pelvis with fused acetabulum articulation and posteriorly oriented ilium, are reminiscent of basal mosasauroids, that are plesiopedal and plesiopelvic “aigialosaurids” and tethysaurines, as well as yaguarasaurines, whose appendicular condition remains mostly unknown (e.g. Palci *et al.*, 2013; Zietlow *et al.*, 2023). In the details, however, *Garamaudo* differs from all these taxa as follows.

The pythonomorph *Mesoleptos* (Lee & Scanlon, 2002) shares with *Garamaudo* a comparable rib morphology, indicating a probably laterally compressed body, and a humerus with a semi-lunar proximal epiphysis and a long and slender shaft although remaining small. It however differs from *Garamaudo* in a slender and twisted humeral shaft and a stronger vertebral osteosclerosis (Houssaye, 2013a).

Aigialosaurus (*A. dalmaticus* and *A. bucchichi*) is comparable to *Garamaudo* in its long and slender PMU, rib morphology, long and slender humerus, and posteriorly oriented ilium. However, *Aigialosaurus* differs by the ilium bearing a posterior process wide and robust along its length, and a large preacetabular process, as well as by possibly pachyostotic ribs (Dutchak & Caldwell, 2006, 2009).

Komensaurus is comparable to *Garamaudo* in its rib morphology and the posteriorly oriented ilium with short preacetabular process. However, it differs by a pelvis exhibiting a loose acetabular articulation and a pubis shorter and distally fan-shaped (Caldwell & Palci, 2007).

Carsosaurus has a long and slender humerus and a posteriorly oriented ilium comparable to *Garamaudo*. However, it differs from it by the very developed pectoral and deltoid crests of the humerus and by its ribs that are long but regularly convex (Caldwell *et al.*, 1995).

Vallecilosaurus bears a posteriorly oriented ilium, similarly as *Garamaudo*, but its pubis appears shorter (Smith & Buchy, 2008). More comparisons are not possible due to the lack of detailed figures.

Haasiasaurus has a long and slender PMU, a long and slender humerus and a posteriorly oriented ilium as *Garamaudo*. Its PMU, however, differs greatly by a surangular very concave dorsally and bearing a large foramen antero-laterally, a retroarticular process fan-shaped (like in plioplatecarpines) and posteromedially oriented, and a glenoid fossa made equally by the surangular and articular (Polcyn *et al.*, 1999). *Haasiasaurus* differs also from *Garamaudo* in having a pelvis with loose acetabular articulation and vertebrae with a stronger osteosclerosis and some pachyostosis (Polcyn et al., 1999; Houssaye, 2013a).

The yaguarasaurine *Yaguarasaurus* differs from *Garamaudo* in a much deeper PMU, though not well preserved (Páramo-Fonseca, 1994).

The yaguarasaurine *Russellosaurus* has a PMU comparable in general shape to *Garamaudo*, notably in its long and slender morphology, elongated slender coronoid articulation, and glenoid fossa made mostly by the articular, the surangular participating only anteriorly (Polcyn & Bell, 2005). However, it differs by a retroarticular process ovoid and posteroventrally oriented, and a surangular dorsal margin (between the glenoid and coronoid) being shorter and concave (in *Garamaudo* it is longer and straight).

The yaguarasaurine *Romeosaurus* exhibits a PMU long and slender comparable to *Garamaudo*, with notably a surangular bearing a coronoid suture long and slender and a lateral articular suture ‘V’-shaped, as well as a possible very short retroarticular process. It however differs by vertebral hypapophyses with rounded articular surfaces for the intercentra, ribs with rounded heads, and a much shorter and wider humerus (Palci *et al.*, 2013).

The tethysaurine *Tethysaurus* possesses a PMU and a posteriorly oriented ilium comparable in shape to *Garamaudo*. However, it differs by a triangular, longer and obliquely oriented retroarticular process, a pelvis bearing loose acetabular articulation and a pubis shorter and distally fan-shaped (Bardet *et al.*, 2003). Finally, it shows no osteosclerosis (Houssaye & Bardet, 2012).

The tethysaurine *Pannoniasaurus*, a coeval freshwater taxon from Hungary, has very similarly to *Garamaudo* a long and slender PMU, prezygapophyses strongly projected anteriorly, extending well beyond the anterior border of the cotyle, oval headed ribs, relatively flat proximal humeral epiphysis, and ilium with a posterior process long, slender, and posteriorly oriented (Makádi *et al.*, 2012). In the details, however, it differs by a retroarticular process longer, very obliquely oriented and bearing a large foramen, rounded cervical hypapophyses, no zygosphenal foramen, and pelvis with probably loose acetabular articulation.

The Villeveyrac mosasauroid, a possible tethysaurine also from almost coeval freshwater environments of southern France (Garcia *et al.*, 2015), has vertebrae with a morphology very similar to those of *Garamaudo.* Unfortunately, no more material is available for comparisons and the microanatomy is unknown.

In conclusion, *Garamaudo bauciensis* can be referred to the Tethysaurinae (*sensu* Makádi *et al.*, 2012) on the basis of the following characters: mandibular glenoid formed mainly by the articular, cervical synapophyses extending below the ventral border of the centrum, ilium with long and slender posterior process and spoon-shaped preacetabular process overlapping the pubis.

Though retaining several plesiomorphic characters, *Garamaudo* differs however from all basal mosasauroids as shown above, and is unique among tethysaurines, being characterized by the following autapomorphies (detailed in the diagnosis): PMU strongly curved inward in dorsal/ventral view; Surangular with a medial horizontal triangular plateau anterior to the glenoid fossa, followed by a straight *adductor fossa* opened along its length; Retroarticular process extremely short and half-moon shaped, oriented obliquely at about 45°, and prolonged antero-medially by an anteriorly oriented hook; osteosclerotic vertebrae; Ribcage high dorsoventrally and laterally compressed; Humerus long and slender but much smaller than the PMU, indicating a possibly reduced anterior limb; Pubis with a very long and slender anterior process, oriented in the body longitudinal axis.

Phylogenetical Analysis

The analysis recovered 537 600 most parsimonious trees (MPTs) with 632 steps each. A strict consensus tree was generated (CI = 0.2574, HI = 7426, RI = 0.6638) and transposed as a time-scaled tree (Figure 10).

Garamaudo nov. gen & nov. sp. is here recovered as a mosasaurid, and more especially as a Tethysaurinae (*sensu* Makádi *et al.*, 2012).

Tethysaurinae are recovered as sister-group of the Yaguarasaurinae (*sensu* Palci *et al.*, 2013), both being included in an unnamed clade, as a polytomy located at the base of the Mosasauridae, which also includes the subfamilies Halisaurinae, Plioplatecarpinae, Tylosaurinae, Mosasaurinae, as in previous analyses (e.g. Zietlow *et al.*, 2023).

Bremer support values are low for Tethysaurinae (1), Yaguarasaurinae (1) and the unamed clade (2), indicating limited robustness of these groupings in the present analysis.

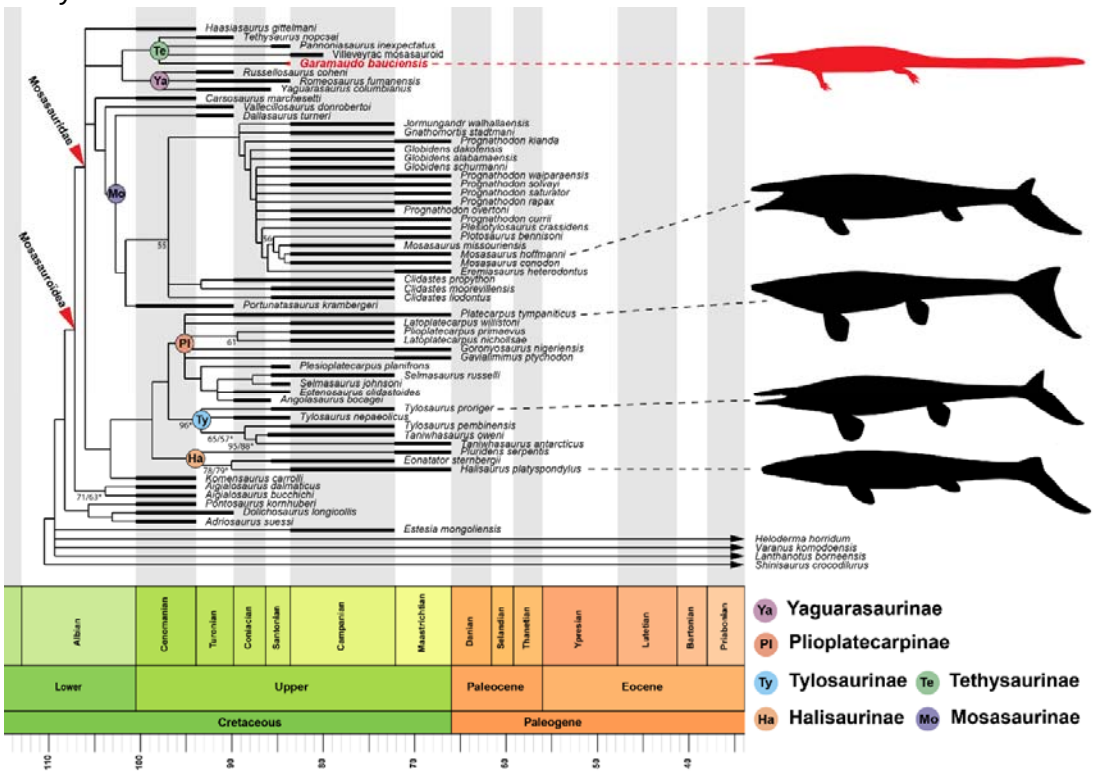

Figure 10. **Time-scaled phylogeny of Mosasauroidea showing the position of *Garamaudo*.** Based on the strict consensus tree obtained from the unweighthed analysis. International Chronostratigraphic Chart after Cohen *et al*. (2013). Temporal occurrences of the extinct taxa are represented as thick black bars whereas extant taxa are indicated with arrows. Node values correspond to bootstrap and jackknife (asterisk) indices, only values equal or superior to 50 percent are indicated. Mosasaurid silhouettes from PhyloPic (http://phylopic.org): *Pannoniasaurus* by Makádi, Caldwell & Ősi (CC BY 4.0); *Platecarpus* by Lindgren, Caldwell, Konishi & Chiappe (CC BY-SA 3.0); *Tylosaurus* by Hartman (CC BY 3.0); *Mosasaurus* by Robinson (CC BY-NC 3.0); Silhouettes of Halisaurinae and *Garamaudo* (modified from *Pannoniasaurus*) designed by F.-L. Pelissier.

The unnamed clade including Tethysaurinae and Yaguarasaurinae is supported by ten unambiguous synapomorphies: parietal table elongate, triangular to subrectangular; narrow postorbitofrontal; postorbitofrontal transverse dorsal ridge present; quadrate suprastapedial process without dorsal constriction; basioccipital canal present; dentary medial parapet elevated and straplike; surangular-articular suture at the middle of the glenoid fossa in lateral view; synapophyses extending far below the ventral margin of the centrum; type 2 vascularization in the basisphenoid ; type 2 basioccipital, with the posteromedial canal entering the basisphenoid between the carotid artery path and the abducens nerve exit.

Yaguarasaurinae *sensu* Palci *et al.* (2013) includes *Yaguarasaurus*, *Russellosaurus* and *Romeosaurus* as a polytomy. They are supported by four unambiguous synapomorphies: frontal not invaded by the posterior end of the nares; long, distinctly below midheight, quadrate suprastapedial process; shallow quadrate alar concavity;

ectopterygoid process of the pterygoid offset anterolaterally and bearing longitudinal grooves and ridges.

Tethysaurinae *sensu* Makádi *et al.* (2012) includes *Tethysaurus*, *Pannoniasaurus*, *Garamaudo* and the Villeveyrac mosasauroid, also as a polytomy. They are supported by seven unambiguous synapomorphies: premaxilla arcuate anteriorly; low median frontal dorsal keel; frontal with discrete ornamentations; 17–19 dentary teeth; humerus ectepicondyle present; humerus entepicondyle present; short retroarticular process relative to glenoid.

Among tethysaurines, *Garamaudo bauciensis* nov. gen. & nov. sp., bears one unambiguous apomorphy: condyle of posterior trunk vertebrae slightly compressed. However, the analysis fails to resolve its position relative to other tethysaurines. This poor resolution could result from the incompleteness of most of these basal taxa.

Discussion

Paleobiology

On the basis of the preserved bones of *Garamaudo*, its size is estimated to about 2.5 m long. Notably, its PMU and vertebrae are comparable in size to those of *Tethysaurus*, estimated to be less than 3 m long (Bardet *et al*.., 2003). The Villeveyrac mosasauroid, a possible tethysaurine, was also estimated to be around 3 m long (Garcia *et al*., 2015). Only *Pannoniasaurus* appears larger, having been estimated as a medium-size tethysaurine of maximum 6 m long (Makádi *et al.*, 2012).

Palci *et al*. (2013) mentioned that, as basal mosasauroids ("aigialosaurids"), *Tethysaurus* and *Pannoniasaurus* retain the plesiopedal and plesiopelvic conditions. This also applies to *Garamaudo* and to the Villeveyrac mosasauroid (Garcia *et al*., 2015), given the morphology of their preserved limb bones.

Osteosclerosis is observed in the vertebrae, ribs and humerus of *Garamaudo*. The vascularization consists in simple vascular canals. It is quite limited to a few canals in the cervical vertebrae and much denser in the dorsal vertebra CD13-PAL.2018.3.4. Conversely, a few simple vascular canals occur in the largest modern terrestrial squamates, whereas all others do not show any vascularization (Buffrénil *et al.*, 2008; Houssaye *et al.*, 2010). In *Garamaudo*, vascularization appears rather similar to what is observed in some pythonomorph lizards such as the marine varanoid *Pachyvaranus* (Buffrénil *et al.*, 2008), the "pythonomorph from Touraine" (Houssaye *et al.*, 2010), or the ophiodomorph *Carentonosaurus* (Houssaye *et al.*, 2008). It is, however, clearly lower than in mosasaurids (Houssaye & Bardet, 2012), even than in the plesiopedal *Dallasaurus*, with moreover the apparent absence of primary osteons in *Garamaudo*, whereas they occur in these mosasaurids. *Garamaudo* growth speed and, by extrapolation, metabolism were therefore probably similar as in pythonomorphs showing a similar vascularization pattern and were thus probably more active than in modern lizards but much lower than in the supposedly gigantothermic mosasaurids (see Houssaye, 2013b).

Vertebral compactness of *Garamaudo* appears lower than in *Carentonosaurus*, *Pachyvaranus*, the pythonomorph from Touraine, *Mesoleptos* and *Haasiasaurus*

(Houssaye, 2013a), but much higher than in the non-marine pythonomorph from Lo Hueco (Houssaye *et al.,* 2013a) and in mosasaurids (Houssaye & Bardet, 2012). Similarly, the rib compactness is lower than that of *Carentonosaurus* and of the ophidiomorph *Pontosaurus*, but much higher than in mosasaurids (Houssaye, 2013a). The humerus is strongly osteosclerotic, to a similar or higher extent than that of *Dallasaurus* (only plesiopedal mosasauroid for which a humerus section is available, to our knowledge; Houssaye *et al.*, 2013b).

There is thus clear osteosclerosis in all studied bones of *Garamaudo* and thus a hydrostatic control of buoyancy and body trim (Houssaye, 2009), which suggests an animal diving at shallow depths with possibly limited acceleration and maneuverability capacities, possibly indicating an ambush predator. This osteosclerosis appears also incompatible with a terrestrial locomotion, because of high fracture risk, despite possible suggestions from the plesiopedal and plesiopelvic conditions of its appendicular skeleton. *Garamaudo* was probably an autochtonous taxon, living in the local freshwater environment (see below). The plesiopedal and plesiopelvic conditions also suggests that its mode of swimming was probably mainly anguilliform (e.g. Lindgren *et al.*, 2011).

Finally, astonishingly, it is worth noting the long and almost straight ribs indicating a laterally compressed, longer than wide, body, and the proportionally small humerus (though remaining plesiomorphically long and slender), suggesting a possible reduced forelimb. The only element of *Garamaudo* permitting to estimate the humerus length compared to the animal size is the PMU. For this purpose, a ratio humerus length / PMU length was calculated. Unfortunately, very few ophidiomorphs and basal mosasauroids preserved both elements. The ratio of *Garamaudo* (0.55) is comparable to that of *Haasiasaurus* (0.53) but stays much lower than in others basal mosasauroids like *Aigialosaurus dalmaticus* (0.63) and *A. bucchichi* (0.87). It is rather similar to that of ophiodomorphs like *Pontosaurus kornhuberi* (0.59) and higher than that of *Pontosaurus lesinensis* (0.37). This makes the proportions of the humerus of *Garamaudo* rather consistent with those observed in these other plesiopedal taxa. The ribs and humerus proportions are moreover reminiscent of the pythonomorph *Mesoleptos* and further enhance the uniqueness of *Garamaudo* among mosasaurids.

Paleoenvironment

The Bouc-Bel-Air - Sousquières locality (BBAS) represents a freshwater ecosystem within the continental deposits of the Aix-en-Provence Basin (Babinot & Durand, 1980; Tortosa & Leleu, 2021).

Its molluscan assemblage closely mirrors classical Valdonnian–basal Fuvelian faunas from Provence (Fabre-Taxy, 1951), dominated by *Melania*-type thiarids and *Hadraxon* that both indicate shallow, low-energy lacustrine to palustrine environments with organic-rich muds favoring the preservation of articulated vertebrate skeletons (Fabre-Taxy, 1951; Babinot & Durand, 1980; Cavin *et al*., 2020; this study). *Viviparus bosquiana* and *Cyanocyclas cuneata* typically occur along vegetated lake margins, implying clear, bicarbonate-rich waters, whereas *Corbicula* species inhabit quiet, sometimes poorly oxygenated floodplain ponds with episodic eutrophic conditions, consistent with shell concentrations at marl–limestone interfaces (Fabre-Taxy, 1951). Altogether, this assemblage points to a moderately eutrophic, carbonate-producing freshwater lake periodically influenced by flooding and shallowing events. Such a rather

rapid flooding episode could explain the state of preservation of the holotype specimen of *Garimaudo*, that includes broken bones but with well-preserved surfaces. This setting contrasts with the marshier, lignite-rich upper Fuvelian faunas of the Gardanne coal Basin, reflecting more humid, swampy environments (Fabre-Taxy, 1951; Babinot & Durand, 1980; Tortosa & Leleu, 2021).

The vertebrate assemblage of BBAS includes the ambush actinopterygian predator *Atractosteus* cf. *africanus* (~2 m; Cavin *et al*., 1996, 2020; « lepisosteidae indet. » in Tortosa, 2014), the benthic coelacanth *Axelrodichthys megadromos* (~1 m; Cavin *et al*., 2020), bothremydid turtle cf. *Polysternon* sp. (~60 cm), small indeterminate crocodylomorphs, and *Garamaudo*, a mid-sized mosasauroid (~2.5 m).

As in the Lower Campanian of Villeveyrac locality (Garcia *et al*., 2015), no large crocodylomorphs are known from BBAS or equivalent Valdonnian–lower Fuvelian localities in Provence (Cavin *et al*., 1996; Tortosa, 2014; Cavin *et al*., 2020). *Garamaudo* therefore ranks among the largest predatory vertebrates in the assemblage, together with *Atractosteus*. Although its precise diet remains unknown, *Garamaudo* may have fed on small fishes, reptiles and/or amphibians, either by active predation or scavanging (Figure 11).

In younger Fuvelian lignite levels, the emergence of medium-sized crocodylomorphs (*Massaliasuchus* and *Allodaposuchus*-like forms) is associated with a marked shift in the fish fauna, which becomes dominated by smaller actinopterygians such as *Lepisosteus* sp. (Martin & Buffetaut, 2008; Tortosa, 2014). At the same time, mosasauroids are no longer recorded in these deposits, whereas other aquatic predators, including hybodontid sharks, appear (Tortosa, 2014; Valentin et al., 2025).

The trophic structure of BBAS parallels that of the Hungarian site of Iharkút, where *Pannoniasaurus*, a tethysaurine mosasaurid closed to *Garamaudo* (see Phylogeny), coexisted with bothremydid turtles, small crocodiles, and gar-like fishes within a freshwater meandering system (Makádi *et al*., 2012). BBAS locality thus represents the second westernmost known equivalent of these continental freshwater ecosystems in Europe during the Santonian, showing that mosasauroids could successfully share top-predator niches in lacustrine-palustrine environments.

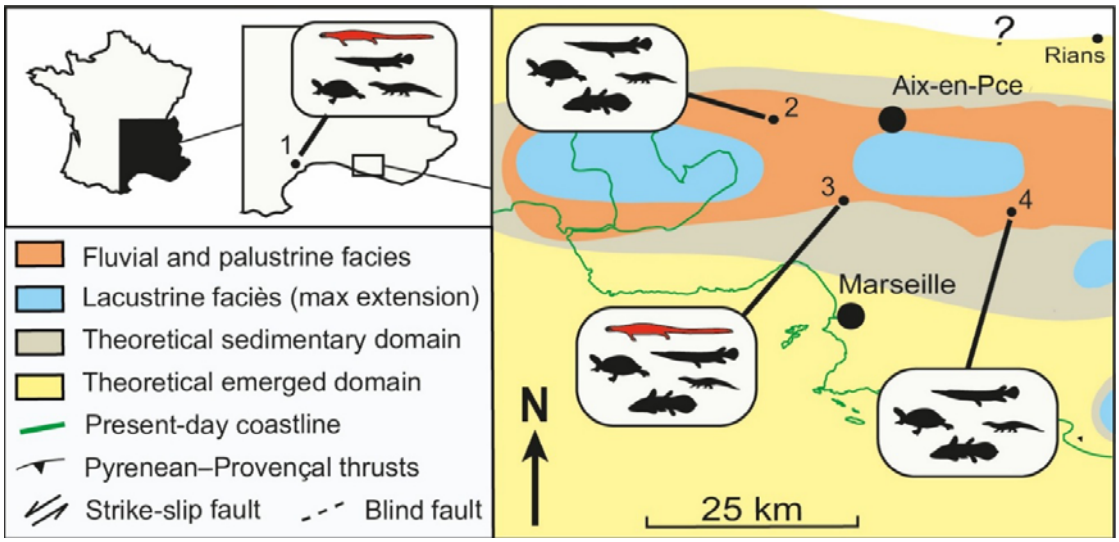

Figure 11 - Paleogeographic reconstruction maps of Provence continental deposits during the latest Santonian (Valdonnian facies), after Tortosa & Leleu (2021), with indications of the main vertebrate outcrops and their faunal content (larger vertebrates only). **1**, Villeveyrac (Languedoc, early Campanian, Garcia *et al*., 2015); **2**, Ventabren (Cavin *et al*., 2020) ; **3**, Bouc-Bel-Air (Cavin *et al*., 2020; this study) ; **4**, Belcodène (Tortosa, 2014). See Figure 2 for the silhouette legend.

Palaeoecology

Modern squamates are known to occupy a wide range of habitats, and even of aquatic habitats, from purely marine to continental ones, passing by estuarine, mangrovial, brackish, and fresh-water environments (Carrillo *et al*., 2024; Neill, 1958). Single species can also exploit various environments alternatively, switching from one to another for either food supply, reproductive purposes or to escape predators, as observed in some Southeast Asian island species of *Varanus* (Pianka & King, 2004). Similarly, also in archosaurs, *Crocodilus porosus*, the only “true” marine living crocodile, is also encountered in estuarine, brackish, and swampy habitats and can be found far inland in freshwater environments (Webb *et al*., 2010). Extant marine reptiles are thus able to occupy an extended range of aquatic environments, attesting of their adaptability, especially in terms of salinity rates.

As for mosasauroids, the oldest (Cenomanian-Turonian) forms (“aigialosaurids”), although exhibiting limited morphological adaptations to an aquatic lifestyle, have all been found in coastal marine environments (Palci *et al.*, 2008), suggesting that the clade rapidly evolved from continental - either being terrestrial or freshwater - squamates into marine forms at this time. Turonian mosasaurids, that include tethysaurines (*Tethysaurus*), yaguarasaurines *(Yaguarasaurus*, *Russellosaurus*, *Romeosaurus*) and early mosasaurines (*Dallasaurus*), were also encountered in marine or estuarine environments (e.g. Polcyn *et al.*, 2025). From the Coniacian–Santonian onward, mosasaurids underwent a progressive shift toward more open-sea conditions until their extinction (e.g. Bardet *et al.*, 2014; Polcyn *et al.*, 2014, 2025). Mosasauroids have thus generally been considered marine taxa. However, this has been challenged by rather recent discoveries of continental tethysaurine mosasauroid remains.

Among tethysaurines, whereas the Turonian *Tethysaurus* was found in clearly marine environment (see Bardet et al., 2003), the Santonian *Pannoniasaurus* as well as the early Campanian Villeveyrac mosasauroid, were found in predominantly freshwater continental ecosystems (Makádi *et al*., 2012; Garcia *et al*., 2015). Tethysaurine isolated teeth were also reported from Turonian and Coniacian freshwater ecosystems of Austria (Ősi *et al*., 2019, 2021). The attribution of *Garamaudo* to tethysaurines thus illustrates an additional occurrence of a freshwater mosasauroid within this clade. Interestingly, in the current state of knowledge, this mosasaurid subfamily is thus the only one which evolved freshwater species. The lack of within-group phylogenetic resolution, however, prevents us from discussing the possibility of only a single or multiple ecological shifts in this lineage, but the above mentioned occurrence of Turonian freshwater tethysaurines (Ősi *et al*., 2019) suggests that during the early stages of their evolution, both marine and freshwater tethysaurines coexisted.

Although the occurrence of these taxa in freshwater deposits could only represent excursions from marine environments, the absence of remains of these taxa in marine deposits and the presence of so far three species in such ecological contexts reinforce

the likelihood of autochtonous freshwater species. The relative ecological plasticity observed in modern aquatic reptiles could explain the establishment of freshwater tethysaurines across the Late Cretaceous European archipelago, allowing them to exploit a mosaic of new ecological niches, facilitated by the absence of large crocodylomorphs, the usual apex-predators of these continental ecosystems (Kocsis *et al.*, 2009; Makádi *et al.*, 2012; see above). Freshwater tethysaurines may also have found refuges inland, facilitating ecological niche partitioning and thereby reducing direct competition with large (> 5 m) coeval marine mosasaurids that became increasingly abundant at this time, including in the European archipelago (e.g. Plasse *et al.*, 2024; Polcyn *et al.*, 2025).

As already mentioned, all tethysaurines known up to now retain the plesiopedal and plesiopelvic conditions. Except *Tethysaurus*, all have been found in continental freshwater environments. And, except *Pannoniasaurus*, all are reduced in size, being no more than 3 m long. The freshwater environment could thus have acted as a physical driver inducing that, globally, small sizes and plesiomorphic limbs and girdles were retained among this basal mosasaurid clade.

Conclusion

New mosasauroid cranial and postcranial remains discovered in the Santonian of Provence, southeastern France, are attributed to a new tethysaurine mosasaur: *Garamaudo bauciensis* nov. gen., nov. sp. The Bouc-Bel-Air - Soucquières (BBAS) locality corresponds to a carbonate-producing freshwater lake and represents the second most westerly continental freshwater ecosystem known in Europe. *Garamaudo* is an about 2.5 meters long mosasaurid with a plesiopedal and plesiopelvis morphology and displays osteosclerosis in its vertebrae, ribs, and humerus (at least). The sedimentological, anatomical and microanatomical data, as well as its estimated intermediate growth rate and thus metbolism as compared to other mosasaurids, are consistent with a rather anguilliform swimmer foraging underwater at shalow depths.

The assignment of this new freshwater mosasaurid to the tethysaurines highlights an additional occurrence of a freshwater species in this taxon and the fact that, based on current knowledge, it is only within the Tethysaurinae that freshwater forms evolved. During the same period, hydropedal and hydropelvic mosasaurs with a higher growth rate and spongious bones illustrating a more active carangiform swimming mode evolved in open marine environments and spread throughout the world. This new discovery therefore contributes to a better understanding of a more diverse and complex evolution with more niche partitioning than previously expected in mosasaurids after the Turonian.

Acknowledgments

We gratefully acknowledge the *Département des Bouches-du-Rhône* and J.-M. Perrin, its elected representative for the promotion of Provence's paleontological and archaeological heritage, for their continuous support, excavation authorization, and administrative assistance. We are also indebted to the *Direction de l'Environnement, des*

Grands Projets et de la Recherche (E. Mangion, H. Souan, M. Bourrelly) and to the *Direction des Routes et des Ports* (F. Cauvin, C. Maréchal, B. Ott, A. Hémery, P. Abignoli) for their help in the field and logistical coordination. We further thank the staff of the *Muséum d'Histoire Naturelle d'Aix-en-Provence* (S. Berton, M. Desparoir, N. Vialle). We acknowledge the MRI platform member of the national infrastructure France-BioImaging supported by the French National Research Agency (ANR-10-INBS-04, «Investments for the future»), the labex CEMEB (ANR-10-LABX-0004) and NUMEV (ANR-10-LABX-0020) and notably R. Lebrun for facilitating access to and use of the µCT. We also warmly thank V. Fischer (Liège University, Belgium) for helpul discussions on the Bremer support indices, as well as P. Loubry (CR2P, Paris) and A. Lethiers (ISTeP / CR2P, Paris) for respectively the photographs and drawings / design of the *Garamaudo* figures.

References

Augusta BG, Zaher H, Polcyn MJ, Fiorillo AR, Jacobs LL (2022) A Review of Non-Mosasaurid (Dolichosaur and Aigialosaur) Mosasaurians. The Origin and Early Evolutionary History of Snakes, vol 90, 157.

Babinot J-F, Durand J-P (1980) Les étages français et leurs stratotypes : Valdonnien, Fuvélien. *Mémoire du BRGM*, 109 : 171–178.

Bardet N, Pereda Suberbiola X, Jalil N-E (2003) A new mosasauroid (Squamata) from the Late Cretaceous (Turonian) of Morocco. *Comptes Rendus Palévol*, 2 (8), 607-616.

Bardet N, Falconnet J, Fischer V, Houssaye A, Jouve S, Pereda Suberbiola X, Perez-Garcia A, Rage J-C, Vincent P (2014) Mesozoic marine palaeobiogeography in response to drifting plate. *Gondwana Research*, 26, 869-887.

Bardet N, Fischer V, Jalil N-E, Khaldoune F, Khadiri-Yazami O, Pereda-Suberbiola X, Longrich N (2025) Mosasaurids Bare the Teeth: An Extraordinary Ecological Disparity in the Phosphates of Morocco Just Prior to the K/Pg Crisis. *Diversity*, 17(114), &-47.

Bell GL Jr (1997) A phylogenetic revision of North American and Adriatic Mosasauroidea. In Ancient marine reptiles (pp. 293-332). Academic Press.

Bell GL, Jr & Polcyn MJ (2005) *Dallasaurus turneri*, a new primitive mosasauroid from the Middle Turonian of Texas and comments on the phylogeny of Mosasauridae (Squamata). *Neth. J. Geosci.* 84, 177–194.

Bell MA, Lloyd GT (2015) Strap: an R package for plotting phylogenies against stratigraphy and assessing their stratigraphic congruence, vol. 58, No. 2, pp. 379-389.

de Buffrénil V, Houssaye A, Böhme W (2008) Bone vascular supply in monitor lizards (Squamata: Varanidae): influence of size, growth, and phylogeny. *Journal of Morphology*, 269(5), 533-543.

Caillol C, Gaviglio P, Durand M (1988) Étude géologique du bassin minier de Gardanne. Rapport BRGM, unpublished, 124 p.

Caldwell MW (2006) A new species of *Pontosaurus* (Squamata, Pythonomorpha) from the Upper Cretaceous of Lebanon and a phylogenetic analysis of

Pythonomorpha. *Mem. Soc. It. Sci. Nat. Museo Civico di Storia Naturale di Milano*, 34, (3), 39 pp.

Caldwell MW, Palci A (2007) A new basal mosasauroid from the Cenomanian (U. Cretaceous) of Slovenia with a review of Mosa sauroid phylogeny and evolution. *J. Vertebrate Paleont.,* 27, (4), 863-880.

Caldwell MW, Carroll RL, Kaiser H (1995) The Pectoral Girdle and Forelimb of *Carsosaurus marchesetti* (Aigialosauridae), with a Preliminary Phylogenetic Analysis of Mosasauroids and Varanoids. *Journal of Vertebrate Paleontology*, 15(3), 516-531.

Carrillo E, Cruz M, Kong B, Mehta RS (2024) Life aquatic: a review of adaptations in non-avian reptiles. eLS, Encyclopedia of life science. Wiley, Hoboken, 1-15.

Cavin L, Martin M, Valentin X (1996) *Atractosteus* (Lepisosteidae, Actinopterygii) du Crétacé supérieur du sud de la France : implications paléobiogéographiques. *Revue de Paléobiologie,* 15(1), 1–17.

Cavin L, Buffetaut E, Dutour Y, Garcia G, Le Loeuff J, Méchin A, Méchin P, Tong H, Tortosa T, Turini E, Valentin X (2020) The last known freshwater coelacanths: new Late Cretaceous mawsoniid remains (Osteichthyes: Actinistia) from southern France. *PLOS ONE*, 15(5), e0233117.

Cohen KM, Finney SC, Gibbard PL, Fan J-X (2013) The ICS International Chronostratigraphic Chart. Episodes 36, 199-204.

Cojan I, Moreau M-G (2006) Correlation of terrestrial climatic fluctuations with global signals during the Upper Cretaceous–Danian in a compressive setting (Provence, France). *Journal of Sedimentary Research*, 76: 589–604.

Collot L (1890) Description du terrain crétacé dans la partie de la Basse-Provence. *Bulletin de la Société Géologique de France*, 3e série, 19, 91 p.

Cope ED (1869) On the reptilian orders Pythonomorpha and Strepto sauria. *Proc. Boston Soc. Nat. Hist.,* 12, 250-266.

Darlu P, Tassy P, D’Haese C, Bagils RZI (2019) La reconstruction phylogénétique (2e éd.). Editions Matériologiques, Paris, 430.

Debraga M, Carroll RL (1993) The origin of mosasaurs as a model of macroevolutionary patterns and processes. *Evolutionary Biology*, 27, 245-322.

Dufaure P, Leguillette J, Vetter P (1967) Coupe de deux sondages forés dans la région de Gardanne (Bouches-du-Rhône). *Bulletin de la Société Géologique de France*, 5 : 25–39.

Durand J-P, Guieu G (1980) Cadre structural du bassin de l'Arc (Bouches-du-Rhône). Revue de l'Industrie Minérale, supplément au numéro de juin 1980 : 13–25.

Dutchak AR, Caldwell MW (2006) Redescription of *Aigialosaurus dalmaticus* Kramberger, 1892, a Cenomanian mosasauroid lizard from Hvar Island, Croatia. *Can. J. Earth Sci.*, 43, 1821-1834.

Dutchak AR, Caldwell MW (2009) A redescription of *Aigialosaurus* (=*Opetiosaurus*) *bucchichi* (kornhuber,1901) (Squamata: Aigialosauridae) with comments on mosasauroid systematics. *Journal of Vertebrate Paleontology* 29(2), 437–452.

Fabre-Taxy S (1951) Faunes lagunaires et continentales du Crétacé supérieur de Provence II – Le Campanien fluvio-lacustre. *Annales de Paléontologie*, 37, 75 p.

Garcia G, Bardet N, Houssaye A, Pereda-Suberbiola X, Valentin X (2015) Mosasauroid (Squamata) discovery in the Late Cretaceous (Early Campanian) continental deposits of Villeveyrac–L'Olivet, southern France. *Comptes Rendus Palevol*, 14(6-7), 495-505.

Gauthier JA, Kearney M, Maisano JA, Rieppel O, Behlke AD (2012) Assembling the squamate tree of life: perspectives from the phenotype and the fossil record. *Bulletin of the Peabody Museum of Natural History*, 53(1), 3-308.

Gaviglio P (1985) A fault and stress field analysis in a coal mine (Gardanne, Bouches-du-Rhône, France). *Tectonophysics*, 113, 349–367.

Gervais P (1852) Zoologie et paleontologie françaises (animaux vertebres): nou velles recherches sur les animaux vivants del la France. Arthus Bertrand.

Gonzalez J (1990) Projet d'information du grand public sur le bassin minier de Gardanne (Bouches-du-Rhône) : le gisement, nature, géométrie, qualité. Rapport BRGM, unpublished, 78 p.

Gradstein FM, Ogg JG, Schmitz MB, Ogg GM (2020) The Geologic Time Scale2012. Elsevier Science & Technology.

Guieu G (1968) Étude tectonique de la région de Marseille. Thèse de Doctorat, Faculté des Sciences de Marseille, 348 p.

Hoffstetter R, Gasc J (1968) Vertebrae and ribs of modern reptiles. Gans, C. & Parsons, T.(Eds.). Biology of the Reptilia New York. 258-490.

Holmes R, Caldwell MW, Cumbaa SL (1999) A new specimen of *Plioplatecarpus* (Mosasauridae) from the lower Maastrichtian of Alberta: comments on allometry, functional morphology, and paleoecology. *Canadian Journal of Earth Sciences*, *36*(3), 363-369.

Honoré A (1938) Révision du Valdonnien et du Fuvélien. Mémoire de D.E.S., Faculté des Sciences de Marseille, unpublished, 95 p.

Houssaye A (2008) A preliminary report on the evolution of the vertebral microanatomy within mosasauroids (Reptilia, Squamata). In *Proceedings of the second Mosasaur meeting* (pp. 81-89). Hays, Kansas: Fort Hays State University.

Houssaye A (2009) “Pachyostosis” in aquatic amniotes: a review. *Integrative Zoology*, *4*, 325-340.

Houssaye, A (2013a) Palaeoecological and morphofunctional interpretation of bone mass increase: an example in Late Cretaceous shallow marine squamates. *Biological Reviews 88*(1), 117-139.

Houssaye A (2013b) Bone histology of aquatic reptiles: what does it tell us about secondary adaptation to an aquatic life? *Biological Journal of the Linnean Society*, *108*(1), 3-21.

Houssaye A & Bardet, N (2012) Rib and vertebral micro-anatomical characteristics of hydropelvic mosasauroids. *Lethaia*, *45*(2), 200-209.

Houssaye A, de Buffrenil V, Rage JC, Bardet N (2008) An analysis of vertebral ‘pachyostosis’ in *Carentonosaurus mineaui* (Mosasauroidea, Squamata) from the Cenomanian (early Late Cretaceous) of France, with comments on its phylogenetic and functional significance. *Journal of Vertebrate Paleontology*, *28*(3), 685-691.

Houssaye A, Mazurier A, Herrel A, Volpato V, Tafforeau P, Boistel R, de Buffrénil V (2010) Vertebral microanatomy in squamates: structure, growth and ecological correlates. *Journal of Anatomy*, *217*(6), 715-727.

Houssaye A, Bardet N, Rage JC, Suberbiola XP, Bouya B, Amaghzaz M, Amalik M (2011) A review of *Pachyvaranus crassispondylus* Arambourg, 1952, a pachyostotic marine squamate from the latest Cretaceous phosphates of Morocco and Syria. *Geological Magazine*, *148*(2), 237-249.

Houssaye A, Bardet N, Narváez I, Ortega F (2013a) Squamate finding in “Lo Hueco”(late Campanian-early Maastrichtian, Cuenca Province, Spain): the second non-marine pythonomorph lizard. *Paläontologische Zeitschrift*, *87*(3), 415-422.

Houssaye A, Lindgren J, Pellegrini R, Lee AH, Germain D, Polcyn MJ (2013b) Microanatomical and histological features in the long bones of mosasaurine mosasaurs (Reptilia, Squamata)–implications for aquatic adaptation and growth rates. *PLoS One*, *8*(10), e76741.

Kocsis L, Ősi A, Vennemann T, Trueman CN, Palmer MR (2009) Geochemical study of vertebrate fossils from the Upper Cretaceous (Santonian) Csehbánya Formation (Hungary): Evidence for a freshwater habitat of mosasaurs and pycnodont fish. *Palaeogeography, Palaeoclimatology, Palaeoecology*, 280, 532-542.

Laurenti JN (1768) Specimen medicum, exhibens synopsin reptilium emendatam cum experimentis circa venena et antidota reptilium austriacorum. Viennae, 214 pp., 5 tab.

Lee MS (1997) The phylogeny of varanoid lizards and the affinities of snakes. *Philosophical Transactions of the Royal Society of London. Series B: Biological Sciences*, 352(1349), 53-91.

Lee MSY, Scanlon JD (2002) The Cretaceous marine squamate *Mesoleptos* and the origin of snakes. *Bull. Natural History Museum of London (Zoology)*, 68, 131-142.

Lindgren J, Polcyn MJ, Young BA (2011) Landlubbers to leviathans: evolution of swimming in mosasaurine mosasaurs. *Paleobiology*, 37(3), 445-469.

Makádi L, Caldwell MW, Ősi A (2012) The first freshwater mosasauroid (Upper Cretaceous, Hungary) and a new clade of basal mosasauroids. *PLoS One*, 7(12), e51781.

Martin J, Buffetaut E (2008) *Crocodilus affuvelensis* Matheron, 1869 from the Late Cretaceous of Southern France: a reassessment. *Zoological Journal of the Linnean Society* 152, 567-580.

Matheron P (1842) Catalogue méthodique et descriptif des corps organisés fossiles du département des Bouches-du-Rhône et lieux circonvoisins. *Répertoire des Travaux de la Société de Statistique de Marseille*, 6, 269 p.

Matheron P (1878) Recherches paléontologiques dans le Midi de la France. 15e partie. Terrain tertiaire. Marseille, unpublished and incomplete manuscript kept at the Muséum d'Histoire Naturelle de Marseille.

Mekarski MM (2017) The Origin and Evolution of Aquatic Adaptations in Cretaceous Squamates. Ph.D. Thesis, Department of Biological Sciences, University of Alberta, Edmonton, 467 pp.

Mistral F (1859) *Mirèio, pouèmo prouvençau*. J. Roumanille, Librairie-Editeur, Avignon.

Neill WT (1958) The occurrence of amphibians and reptiles in saltwater areas, and a bibliography. *Bulletin of Marine Science*, 8(1), 1-97.

Oppel M (1811) Die Ordnungen, Familien und Gattungen der Reptilien als Prodrom einer Naturgeschichte derselben. Lindauer, München xii + 87 pp.

Ősi A, Szabó M, Kollmann H, Wagreich M, Kalmar R, Makádi L, Szentesi Z, Summesberger H (2019) Vertebrate remains from the Turonian (Upper Cretaceous) Gosau Group of Gams, Austria. *Cretaceous Research* 99, 190-208.

Ősi A, Szabó M, E Tóth, Bodor E, Lobitzer H, Kvaček J, Svobodova M, Szente I, Wagreich M, Trabelsi K, Sames B, Magyar J, Makádi L, Berning B, Botfalvai G (2021) A brackish to non-marine aquatic and terrestrial fossil assemblage with vertebrates from the lower Coniacian (Upper Cretaceous) Gosau Group of the Tiefengraben locality near St. Wolfgang im Salzkammergut, Austria. *Cretaceous Research* 127, 104938.

Palci A, Caldwell MW (2007) Vestigial forelimbs and axial elon gation in a 95 million-year-old non-snake squamate. *J. Vert. Paleont.,* 27, (1), 1-7.

Palci A, Jurkovšek B, Kolar-Jurkovšek T, Caldwell MW (2008) New palaeoenvironmental model for the Komen (Slovenia) Cenomanian (Upper Cretaceous) fossil lagerstätte. *Cretaceous Research*, *29*(2), 316-328.

Palci A, Caldwell MW, Papazzoni CA (2013) A new genus and subfamily of mosasaurs from the Upper Cretaceous of northern Italy, *Journal of Vertebrate Paleontology*, 33:3, 599-612.

Páramo-Fonseca ME (1994) Posición sistemática de un reptil marino con base en los restos fósiles encontrados en capas del Cretácico superior en Yaguará (Huila). *Rev. Acad. Colomb. Cienc. Ex., Fís. Nat.*, 19, (72), 63-80.

Pianka E, King D (2004) Varanoid lizards of the world. Indiana University Press.

Pierce SE, Caldwell MW (2004) Redescription and phylogenetic position of the Adriatic (Upper Cretaceous; Cenomanian) dolichosaur *Pontosaurus lesinensis* (Kornhuber, 1873). *Journal of Vertebrate Paleontology* 24(2), 373–386.

Plasse M, Valentin X, Garcia G, Guinot G, Bardet N (2024) New remains of Mosasauroidea (Reptilia, Squamata) from the Upper Cretaceous (Santonian) of Aude, southern France. *Cretaceous Research*, 157, 105823.

Polcyn MJ, Bell GLJr (2005) *Russellosaurus coheni* n. gen., n. sp., a 92 million-year-old mosasaur from Texas (USA), and the definition of the parafamily Russellosaurina. *Neth. J. Geosci.* 84, 321–333.

Polcyn MJ, Tchernov E, Jacobs LL (1999) The Cretaceous bio geography of the eastern Mediterranean with a description of a new basal mosasauroid from ’Ein Yabrud, Israel. In: Y Tomida, TH Rich and P Vickers-Rich, Eds, Proc. Second Gondwanan Dinosaur Symposium. National Science Museum Monographs, Tokyo, 15, 259-290.

Polcyn MJ, Jacobs LL, Araújo R, Schulp AS, Mateus, O (2014) Physical drivers of mosasaur evolution. *Palaeogeogr. Palaeoclimatol. Palaeoecol.* 400, 17–27.

Polcyn MJ, Augusta BG, Zaher H, Gower DJ, Zaher H (2022) Reassessing the morphological foundations of the pythonomorph hypothesis. The Origin and Early Evolutionary History of Snakes; Gower, DJ, Zaher, H., Eds, 125-156.

Polcyn MJ, Robbins JA, Schulp AS, Lindgren J, Jacobs LL (2025) The Evolution of Mosasaurid Foraging Behavior Through the Lens of Stable Carbon Isotopes. *Diversity*, *17*(4), 291.

Rieppel O, Zaher H, Tchernov E, Polcyn MJ (2003) The anatomy and relationships of *Haasiophis terrasanctus*, a fossil snake by well-developed hind limbs from the Mid-Cretaceous of the Middle East. *Journal of Paleontology*, *77*(3), 536-558.

Roule L (1886) Nouvelles recherches sur les mollusques du terrain lacustre inférieur de Provence. *Annales de Malacologie*, 2, 195–228.

Russell DA (1967) Systematics and morphology of American mosasaurs. Peabody Museum of Natural History, *Yale University Bull*., 23, 1-240.

Simões T R, Vernygora O, Paparella I, Jimenez-Huidobro P, Caldwell MW (2017) Mosasauroid phylogeny under multiple phylogenetic methods provides new insights on the evolution of aquatic adaptations in the group. *PLoS One*, 12(5), e0176773.

Simões TR, Pyron RA (2021) The squamate tree of life. *Bulletin of the Museum of Comparative Zoology*, *163*(2), 47-95.

Smith KT, Buchy M-C (2008) A new aigialosaur (Squamata: Anguimorpha) with soft tissue remains from the Upper Cretaceous of Nuevo León, Mexico. *Journal of Vertebrate Paleontology,* 28, 85–94.

Strong CR, Caldwell MW, Konishi T, Palci A (2020) A new species of longirostrine plioplatecarpine mosasaur (Squamata: Mosasauridae) from the Late Cretaceous of Morocco, with a re-evaluation of the problematic taxon '*Platecarpus*' *ptychodon*. *Journal of Systematic Palaeontology,* 18(21), 1769-1804.

Swofford DL (2003) PAUP*. Phylogenetic Analysis Using Parsimony (*and Other Methods). Version 4. Sinauer Associates, Sunderland, Massachusetts.

Tortosa T (2014) Vertébrés continentaux du Crétacé supérieur de Provence (Sud-Est de la France). Thèse, Université Pierre et Marie Curie, Paris, unpublished, 462 p.

Tortosa T, Buffetaut E, Vialle N, Dutour Y, Turini E, Cheylan G (2014) A new abelisaurid dinosaur from the Late Cretaceous of southern France: palaeobio-geographical implications. *Annales de Paléontologie* (100), 63–86.

Tortosa T, Leleu S (2021) Les bassins continentaux et la première orogenèse provençale au Crétacé final : du Santonien terminal au Maastrichtien (–85 Ma à –66 Ma). In: Bourrideys, J. (Ed.), Géologie des Bouches-du-Rhône – Roches et paysages remarquables, Éditions BRGM, pp. 87–104.

Valentin X, Vullo R, Cuny G, Jansen O, Garcia G (2025) Hybodont shark remains from Campanian (Upper Cretaceous) continental deposits of southern France. *Cretaceous Research* 177: 106205.

Webb GJ, Manolis SC, Brien ML (2010) Saltwater crocodile *Crocodylus porosus*. Crocodiles. Status Survey and Conservation Action Plan. Third Edition, ed. by SC Manolis and C. Stevenson. Crocodile Specialist Group: Darwin, 99-113.

Westphal M, Durand J-P (1990) Magnétostratigraphie des series continentales fluvio-lacustres du Crétacé supérieur dans le synclinal de l'Arc (région d'Aix-en-Provence, France). *Bull. Soc. géol. France* (8) 4: 609-620.

Zietlow AR, Boyd CA, Van Vranken NE (2023) *Jormungandr walhallaensis*: A new mosasaurine (Squamata: Mosasauroidea) from the Pierre Shale Formation (Pembina Member: Middle Campanian) of North Dakota. *Bulletin of the American Museum of Natural History*, 464(1), 1-82.

Appendix 1 (Phylogeny)

Taxa

Added taxa:
***Garamaudo bauciensis*, nov. gen. nov sp., this work.**

Villeveyrac mosasauroid, scored from the description by Garcia *et al.* (2015).

Vallecillosaurus donrobertoi, scored from the description by Smith & Buchy (2008) and matrix by Mekarski (2017).

Haasiasaurus gittelmani, scored from the description by Polcyn *et al.* (1999) and matrix by Mekarski (2017).

Carsosaurus marchesetti, scored from the description by Kornhuber (1893), Caldwell *et al.* (1995) and matrix by Mekarski (2017).

Portunatasaurus krambergeri, scored from the description by Mekarski *et al.* (2019) and matrix by Mekarski (2017).

Modified taxa:
Shinisaurus crocodilurus modified from Augusta *et al.* (2022). Character 43 (1 → 0).

Heloderma horridum modified from Augusta *et al.* (2022). Character 43 (1 → 0).

Lanthanotus borneensis modified from Augusta *et al.* (2022). Character 43 (1 → 0).

Varanus komodoensis modified using observation of the 3D model TNHC.Herpetology.95803 (Gray, 2024). Character 43 (1 → 0).

Adriosaurus suessi modified from Augusta *et al.* (2022). Character 43 (? → 0).

Pontosaurus kornhuberi modified from Augusta *et al.* (2022). Character 43 (? → 0).

Agialosaurus dalmaticus modified from Augusta *et al.* (2022) and Dutchak & Caldwell (2009). Character 25 (0 →1), character 85 (1 → 0).

Aigialosaurus (= *Opetiosaurus*) *bucchichi* modified from Augusta *et al.* (2022) and Dutchak & Caldwell (2009). Character 25 (0 → 1), character 43 (0 → 1), character 85 (1 → 0), character 86 (? → 0).

Komensaurus carrolli modified from Augusta *et al.* (2022). Character 43 (0 → 1).

Pannoniasaurus inexpectatus modified from Makádi *et al.* (2012). Character 4 (? → 0), character 28 (? → 1), character 37 (0 →) 1; character 43 (0 → 1), character 47 (2 → 0), character 53(0 → ?), character 62 (? → 1), character 63 (? → 0), character 69 (1 → 0), character 70 (1 → ?), character 72 (0 → 1), character 78 (1 → 0), character 79 (1 → 0), character 84 (0 → ?), character 98 (0 → ?), character 99 (1 → ?), character 102 (? → 0), character 103 (? → 0), character 104 (? → 1), character 106 (0 → 1), character 107 (0 → 1).

Tethysaurus nopcsai modified from Bardet *et al.* (2003), Makádi *et al.* (2012), Houssaye & Bardet (2012) and Augusta *et al.* (2022). Character 10 (1 → 0), character 13 (? → 0), character 15 (2 → 3, character 16 (? → 0), character 43 (0 → 1), character 78 (1 → 0), character 79 (1 → 0), character 94 (1 → 0), character 106 (0 → 1), character 107 (0 → 1).

Romeosaurus fumanensis modified from Palci *et al.* (2013). Character 7 (? → 0), character 8 (? → 2).

Pluridens serpentis modified from Longrich *et al.* (2021). Character 15 (? → 3).

Eonatator sternbergi modified from Augusta *et al.* (2022). Character 43 (0 → 1).

Halisaurus platyspondylus modified from Bell (1997). Character 43 (0 → 1).

Characters

Modified character:
40. Quadrate suprastapedial process fusion: absent (0); present with a pillar-like process in some case (1); present with the base of quadrate (2). Based on Palci *et al.* (2021).

Added characters:
125. Caudal vertebrae, depth: Regular, no sculling organ, ratio being 1,4 or less (0); weakly developed sculling organ, ratios varying from 1,5 to 2,5 (1); very deep, forming a strong sculling organ, ratio being 2.6 or higher (2). Based on Augusta *et al.* (2022).

126. Posteromedial canal enters basisphenoid between the carotid artery path and abducens nerve exit: absent (0); present (1). Based on character 98 of Polcyn *et al.* (2023).

127. Vascularization of the basisphenoid and basioccipital: Type 1, no accessory anterolateral foramina or internal canal in the basisphenoid or basioccipital (0); Type

2, posteromedial canal in the basisphenoid present, forming a canal or vestibule in the basisphenoid body, exiting ventrally and does not pass into basisphenoid anteriorly (1); Type 3, posteromedial canal in the basisphenoid present, forming a canal or vestibule in the basisphenoid body, and passes anteriorly into basisphenoid (2). Note: this character is the fusion of characters 99 and 100 of Polcyn *et al.* (2023); states were coded as 0 (inferred) when not observed in Halisaurinae, Mosasaurinae, and Tylosaurinae, following Polcyn *et al.* (2023); states were coded as "?" in dolichosaurids and basal branching mosasauroids, also according to Polcyn *et al*. (2023).

128. Dorsal surface of the frontal bears discrete ornamentations: absent (0); present (1).

129. Retroarticular process length relative to glenoid fossa: elongated (0); short (1); extremely short (2). Note: the length is qualitative here and based on personal observations and descriptions using bibliography. "Elongated" refers to a long, slender retroarticular process, longer than the glenoid fossa (as in outgroups such as varanids); "Short" refers to a curved retroarticular process approximately equal in length to the glenoid fossa (as in most mosasauroids); "Extremely short" refers to a curved retroarticular process distinctly shorter than the glenoid fossa (as in *Garamaudo*).

Outgroup list

Species	Family	Superfamily	Reference
Shinisaurus crocodilurus	Shinisauridae	—	Ahl (1930)
Lanthanotus borneensis	Lanthanotidae	Varanoidea	Augusta *et al.* (2022)
Varanus komodoensis	Varanidae	Varanoidea	Augusta *et al.* (2022)
Heloderma horridum	Helodermatidae	Varanoidea	Augusta *et al.* (2022)
Estesia mongoliensis	—	Varanoidea	Norell *et al.* (1992)
Adriosaurus suessi	« Dolichosauridae »	—	Augusta *et al.* (2022)
Dolichosaurus longicollis	« Dolichosauridae »	—	Augusta *et al.* (2022)

Pontosaurus kornhuberi	« Dolichosauridae »	—	Augusta *et al.* (2022)

Missing data (?) percentage for each taxon

Taxa	Missing data (%)
Vallecillosaurus donrobertoi	90.70
Villeveyrac mosasauroid	86.05
Garamaudo bauciencis	83.72
Goronyosaurus nigeriensis	82.17
Portunatasaurus krambergeri	79.07
Dolichosaurus longicollis	77.52
Prognathodon waiparaensis	73.64
Komensaurus carrolli	72.87
Prognathodon currii	72.09
Carsosaurus marchesetti	71.32
Selmasaurus russelli	69.77
Dallasaurus turneri	67.44
Pluridens serpentis	62.96
Adriosaurus suessi	62.79
Gavialimimus ptychodon	61.24
Mosasaurus conodon	61.24
Gnathomortis stadtmani	56.06
Globidens schurmanni	55.81
Pannoniasaurus inexpectatus	55.04
Yaguarasaurus columbianus	54.26
Romeosaurus fumanensis	54.26
Angolasaurus bocagei	54.26
Prognathodon kianda	53.49
Globidens dakotensis	51.94
Latoplatecarpus nichollsae	51.16
Globidens alabamaensis	51.16
Taniwhasaurus antarcticus	48.84
Taniwhasaurus oweni	48.06
Haasiasaurus gittelmani	48.06
Jormungandr walhallaensis	47.29
Aigialosaurus dalmaticus	44.19
Halisaurus platyspondylus	44.19
Prognathodon saturator	42.64
Russellosaurus coheni	41.09
Estesia mongoliensis	40.15
Pontosaurus kornhuberi	34.88
Selmasaurus johnsoni	34.88
Eremiasaurus heterodontus	34.88
Prognathodon solvayi	32.56
Latoplatecarpus willistoni	31.01
Mosasaurus missouriensis	29.46
Plesiotylosaurus crassidens	28.68
Aigialosaurus bucchichi	27.91
Tethysaurus nopcsai	26.52

Taxa	Missing data (%)
Clidastes propython	20.93
Prognathodon rapax	20.93
Plesioplatecarpus planifrons	20.16
Tylosaurus nepaeolicus	18.94
Plotosaurus bennisoni	18.60
Eonatator sternbergii	17.05
Ectenosaurus clidastoides	16.28
Tylosaurus pembinensis	15.91
Prognathodon overtoni	13.95
Plioplatecarpus primaevus	9.30
Clidastes moorevillensis	6.98
Mosasaurus hoffmanni	3.88
Platecarpus tympaniticus	3.10
Clidastes liodontus	3.03
Lanthanotus borneensis	1.52
Heloderma horridum	1.48
Varanus komodoensis	1.45
Shinisaurus crocodilurus	0.74
Tylosaurus proriger	0.72

References

Ahl E (1930) Beitrage zur Lurch und Kriechtierfauna Kwangsi: Section 5, Eidechsen. *Sitzungsberichte der Gesellschaft der naturforschenden Freunde zu Berlin*, 326-331.

Augusta BG, Zaher H, Polcyn MJ, Fiorillo AR, Jacobs LL (2022) A Review of Non-Mosasaurid (Dolichosaur and Aigialosaur) Mosasaurians. In: The Origin and Early Evolutionary History of Snakes. Cambridge University Press, Cambridge, 157-179.

Bardet N, Pereda Suberbiola X, Jalil NE (2003) A new mosasauroid (Squamata) from the Late Cretaceous (Turonian) of Morocco. *Comptes Rendus Palevol*, 2(8), 607-616.

Bell GLJr (1997) A phylogenetic revision of North American and Adriatic Mosasauroidea. In: Ancient marine reptiles. Academic Press, San Diego, 293-332.

Caldwell MW, Carroll RL, Kaiser H (1995) The Pectoral Girdle and Forelimb of *Carsosaurus marchesetti* (Aigialosauridae), with a Preliminary Phylogenetic Analysis of Mosasauroids and Varanoids. *Journal of Vertebrate Paleontology*, 15(3), 516-531.

Dutchak AR, Caldwell MW (2009) A redescription of *Aigialosaurus* (= *Opetiosaurus*) bucchichi (Kornhuber, 1901) (Squamata: Aigialosauridae) with comments on mosasauroid systematics. *Journal of Vertebrate Paleontology*, 29(2), 437-452.

Garcia G, Bardet N, Houssaye A, Pereda-Suberbiola X, Valentin X (2015) Mosasauroid (Squamata) discovery in the Late Cretaceous (Early Campanian) continental deposits of Villeveyrac–L'Olivet, southern France. *Comptes Rendus Palevol*, 14(6-7), 495-505.

Gray, J (2024) Skull of a Komodo dragon (*Varanus komodoensis*) with colored bones [3D mesh]. Texas Natural History Collections, University of Texas, managed by oVert TCN project. MorphoSource.
https://www.morphosource.org/concern/media/000677422?locale=en

Houssaye A, Bardet N (2012) A baby mosasauroid (Reptilia, Squamata) from the Turonian of Morocco–*Tethysaurus* 'junior'discovered? *Cretaceous Research*, 46, 208-215.

Kornhuber A, (1893) *Carsosaurus marchesettii*, ein neuer fossiler Lacertilier aus den Kreideschichten des Karstes bei Komen. Abhandlungen der K.K. geologischen Reichsanstalt, Wien 17, 1–15., E

Longrich N R, Bardet N, Khaldoune F, Yazami OK, Jalil NE (2021) *Pluridens serpentis*, a new mosasaurid (Mosasauridae: Halisaurinae) from the Maastrichtian of

Morocco and implications for mosasaur diversity. *Cretaceous Research*, 126, 104882.
Makádi L, Caldwell MW, Ősi A (2012) The first freshwater mosasauroid (Upper Cretaceous, Hungary) and a new clade of basal mosasauroids. *PLoS One*, 7(12), e51781.

Mekarski MM (2017) The Origin and Evolution of Aquatic Adaptations in Cretaceous Squamates. Ph.D. Thesis, Department of Biological Sciences, University of Alberta, Edmonton, 467 pp.

Mekarski MC, Japundžić D, Krizmanić K, Caldwell MW (2019) Description of a new basal mosasauroid from the Late Cretaceous of Croatia, with comments on the evolution of the mosasauroid forelimb. Journal of Vertebrate Paleontology, 39(1), e1577872.

Norell M, McKenna MC, Novacek MJ, Akademi MSU (1992) *Estesia mongoliensis*: a new fossil varanoid from the late Cretaceous Barun Goyot Formation of Mongolia. *American Museum novitates*; 3045, 1-24.

Palci A, Caldwell MW, Papazzoni CA (2013) A new genus and subfamily of mosasaurs from the Upper Cretaceous of northern Italy. *Journal of Vertebrate Paleontology*, 33(3), 599-612.

Palci A, Konishi T, Caldwell MW (2021) A comprehensive review of the morphological diversity of the quadrate bone in mosasauroids (Squamata: Mosasauroidea), with comments on the homology of the infrastapedial process. Journal of Vertebrate Paleontology 40 (6), 1–11.

Polcyn MJ, Tchernov E, Jacobs LL (1999) The Cretaceous bio geography of the eastern Mediterranean with a description of a new basal mosasauroid from ’Ein Yabrud, Israel. In: Y. Tomida, T.H. Rich and P. Vickers-Rich, Eds, Proc. Second Gondwanan Dinosaur Symposium. National Science Museum Monographs, Tokyo, 15, 259-290.

Polcyn MJ, Bardet N, Albright III LB, Titus A (2023) A new lower Turonian mosasaurid from the Western Interior Seaway and the antiquity of the unique basicranial circulation pattern in Plioplatecarpinae. *Cretaceous Research*, 151, 105621.